Radio Occultation Measurements in the Cloudy Boundary Layer

[1]Anthony J. Mannucci

[1]Chi Ao

[2]E. Robert Kursinski

[1]Feiqin Xie

[1]Byron Iijima

[1]Dong Wu

[1]Jet Propulsion Laboratory, California Institute of Technology

[2]University of Arizona, Tucson

KISS Workshop

"Innovative Satellite Observations To Characterize The Cloudy Boundary Layer"

September 22, 2010

Overview of Today's Talk

- Measurement concept and recent results
- RO in the boundary layer
- Research directions

The Radio Occultation Measurement

Geometry of an acquisition

Snell's Law

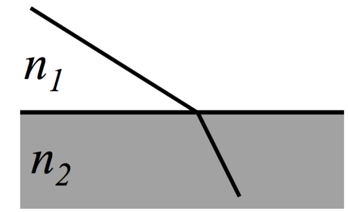

$$N = a_1 \frac{P}{T} + a_2 \frac{P_W}{T^2}$$

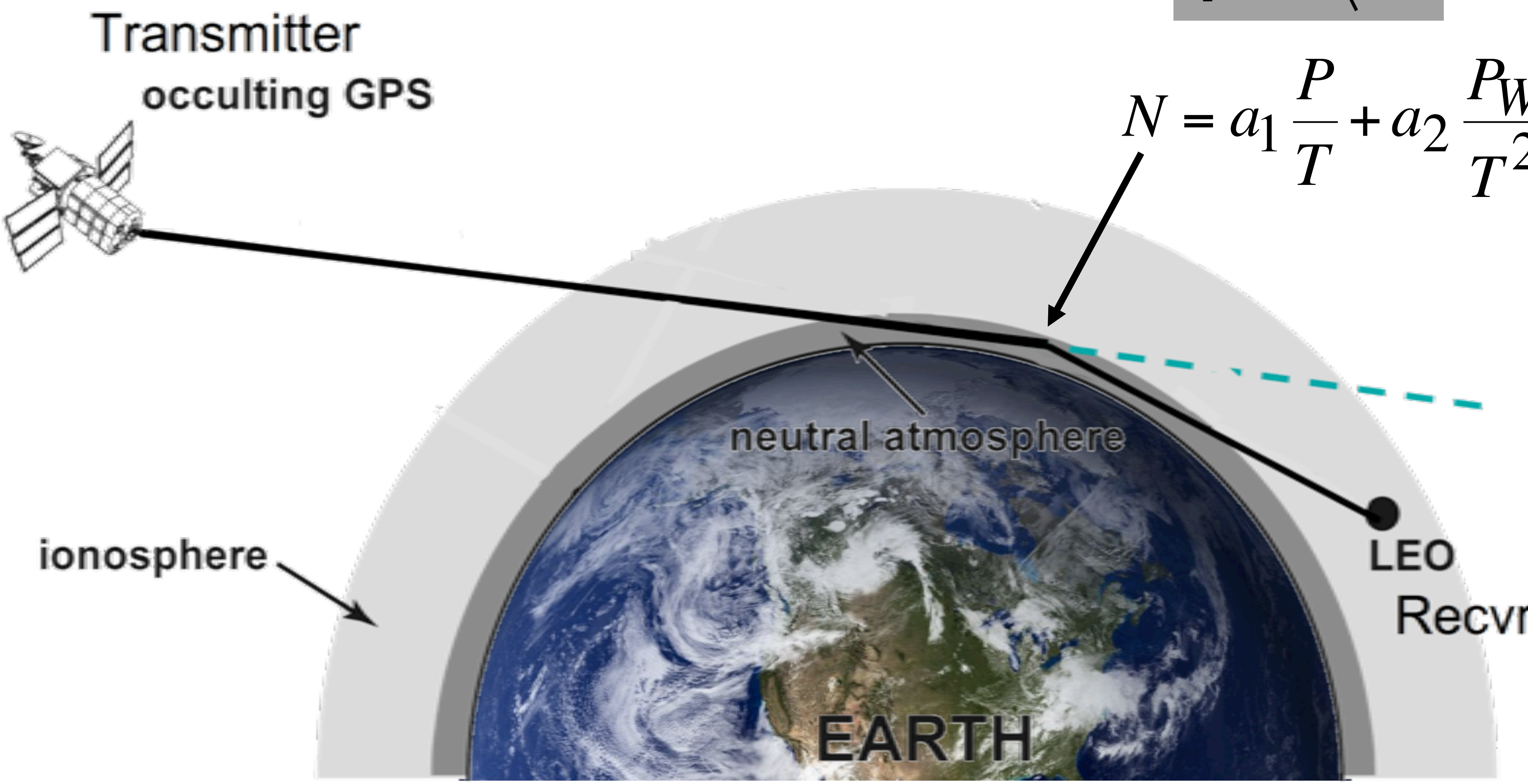

Atmospheric Refractivity at L-band

$$N = (n-1) \times 10^6$$

$$= a_1 \frac{P}{T} + a_2 \frac{P_w}{T^2} - 40.3 \times 10^6 \frac{n_e}{f^2}$$

$$+ O\left(\frac{1}{f^3}\right) + a_w W_w + a_i W_i$$

a_1 =77.6 K/mbar

a_2 =3.73x10^5 K^2/mbar

W_w and W_i are liquid water and ice content (g/m^3)
a_w = 1.4 m^3/g
a_i = 0.6 m^3/g

$$\frac{dP}{dh} = -g\rho$$

$$\rho = \rho_d + \rho_w = \frac{m_d P}{TR} + \frac{(m_w - m_d) P_w}{TR}$$

L1 = 1.575 GHz
L2 = 1.227 GHz

“Onion Skin” Retrieval Approach

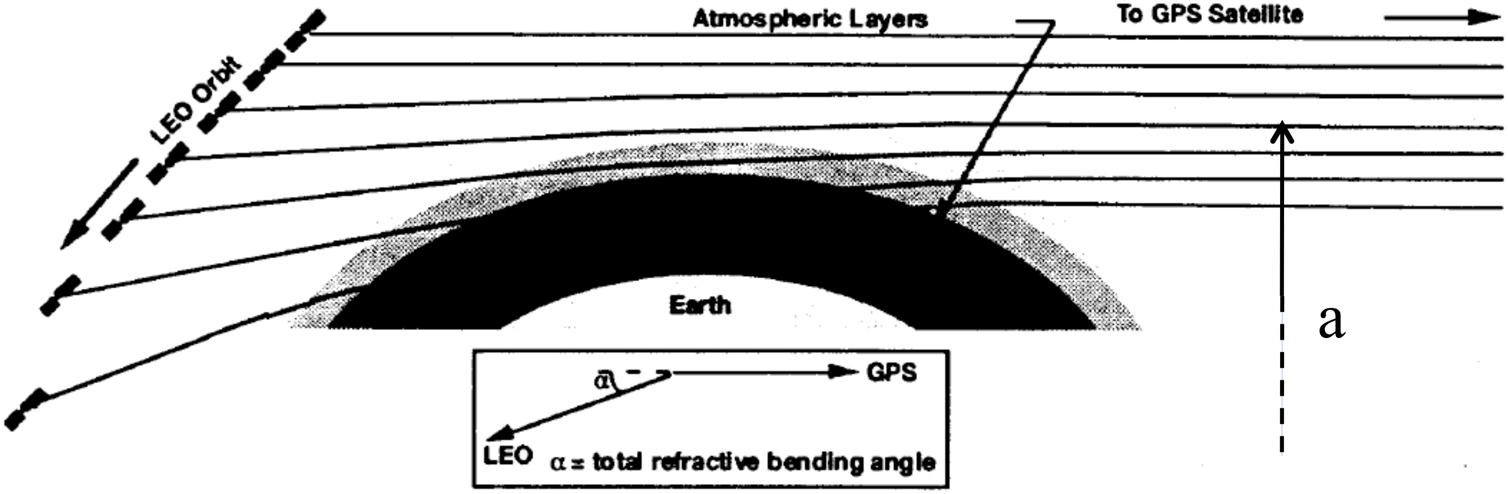

$$\begin{bmatrix} \delta\alpha_1 \\ \delta\alpha_2 \\ \delta\alpha_3 \\ \vdots \\ \delta\alpha_m \end{bmatrix} = \begin{bmatrix} X_{11} & 0 & 0 & \cdots & 0 \\ X_{21} & X_{22} & 0 & \cdots & 0 \\ X_{31} & X_{32} & X_{33} & 0 \cdots & 0 \\ \vdots & & & & \\ X_{m1} & X_{m2} & X_{m3} & \cdots & X_{mm} \end{bmatrix} \bullet \begin{bmatrix} \delta(\nabla n_1) \\ \delta(\nabla n_2) \\ \delta(\nabla n_3) \\ \vdots \\ \delta(\nabla n_m) \end{bmatrix}$$

$$\boxed{\alpha_0 = \nabla n_0 = 0}$$

Spherically symmetric case:

$$\alpha(a) = -2a \int_a^{\infty} \frac{1}{\sqrt{a'^2 - a^2}} \frac{\mathrm{d}\ln(n)}{\mathrm{d}a'} \mathrm{d}a'$$

Abel inversion

$$\ln(n(a)) = \frac{1}{\pi} \int_a^{\infty} \frac{\alpha(a')}{\sqrt{a'^2 - a^2}} \mathrm{d}a'$$

Melbourne et al., JPL Pub 94-18, 1994

Geophysical Retrieval

Doppler Measurement & spherical symm

↓

Bending Angle vs Altitude

↓ ***Abel transform***

Refractivity vs Altitude

↓

Ideal gas, hydrostatic equilibrium

$$N = a_1 \frac{P}{T} + a_2 \frac{P_W}{T^2}$$

$$\frac{dP}{dh} = -\rho g$$

↓

T*, *P* versus *altitude
geopotential height

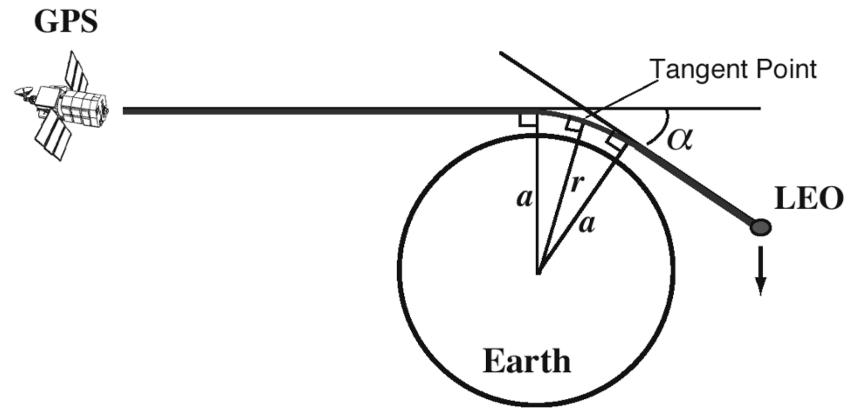

$$\lambda \Delta f = [\mathbf{v}_t \cdot \hat{\mathbf{k}}_t - \mathbf{v}_r \cdot \hat{\mathbf{k}}_r - (\mathbf{v}_t - \mathbf{v}_r) \cdot \hat{\mathbf{k}}]$$

Horizontal resolution: 50-300 km
Vertical resolution: 50m - 1 km

Minimally affected by liquid water, precipitation and ice

Geographical Coverage

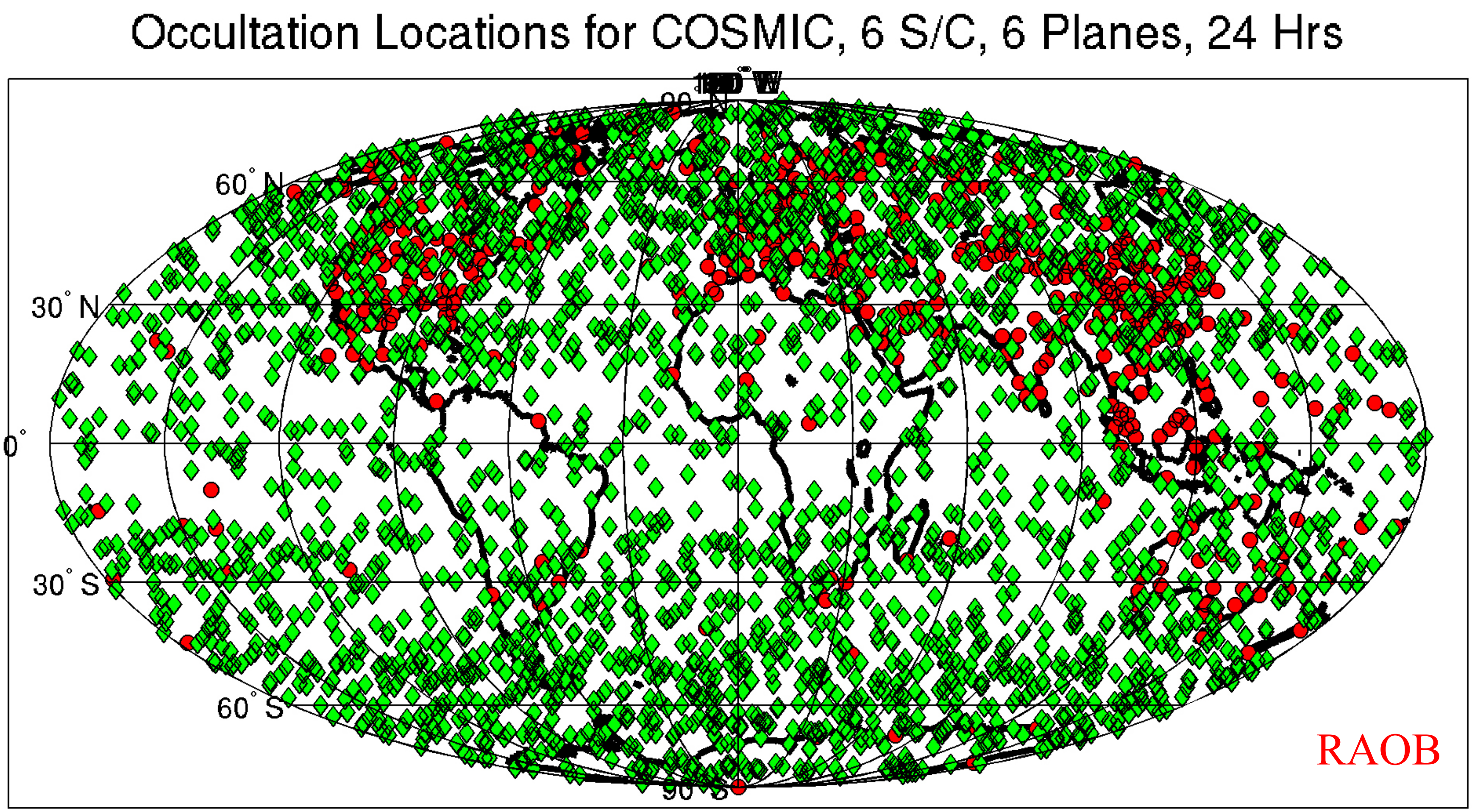

COSMIC-Follow On: 12 satellites, GPS+Galileo, 2014 and 2016

RO versus Radiosonde
High Accuracy and Precision in UTLS

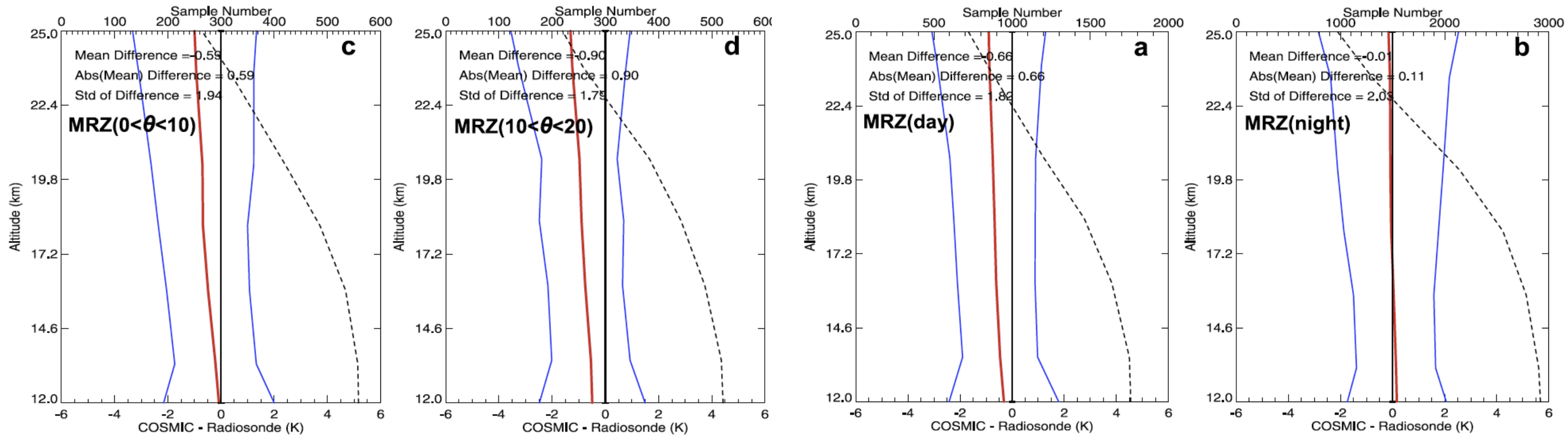

He et al., GRL 2009

- **Multi-year statistical profile comparison**
- **IGRA database**
- **CHAMP RO**

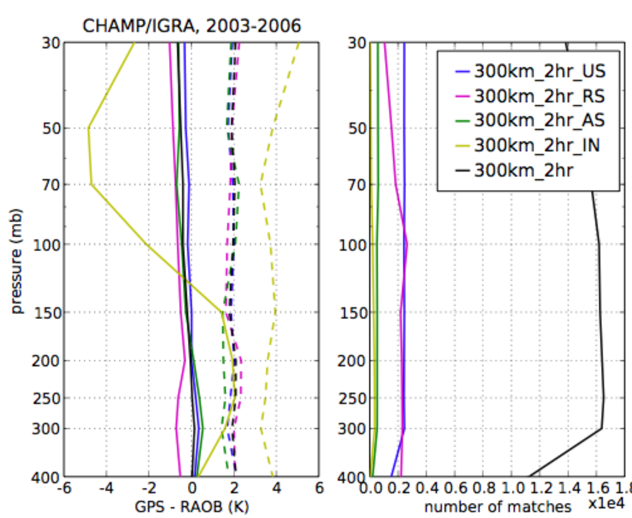

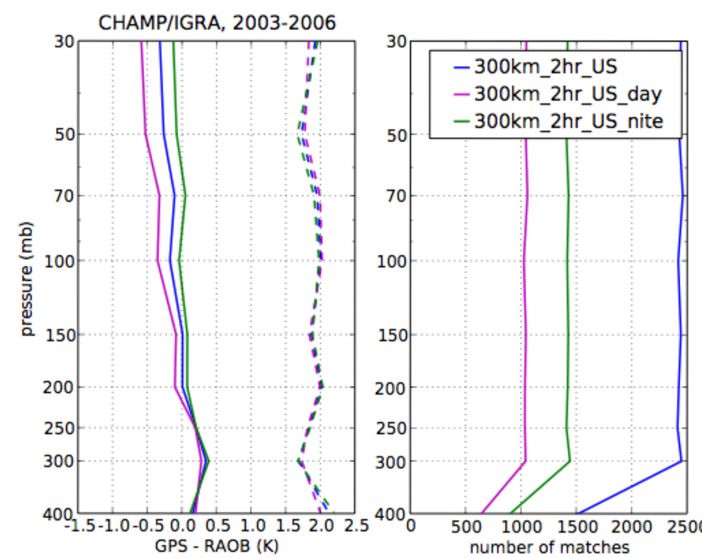

JPL

Continents:

USA

Russia

Australia

India

- Statistically significant difference in daytime versus nighttime means

Water Vapor Retrievals – Uncertainty Estimates

Humidity Versus Temperature Uncertainty

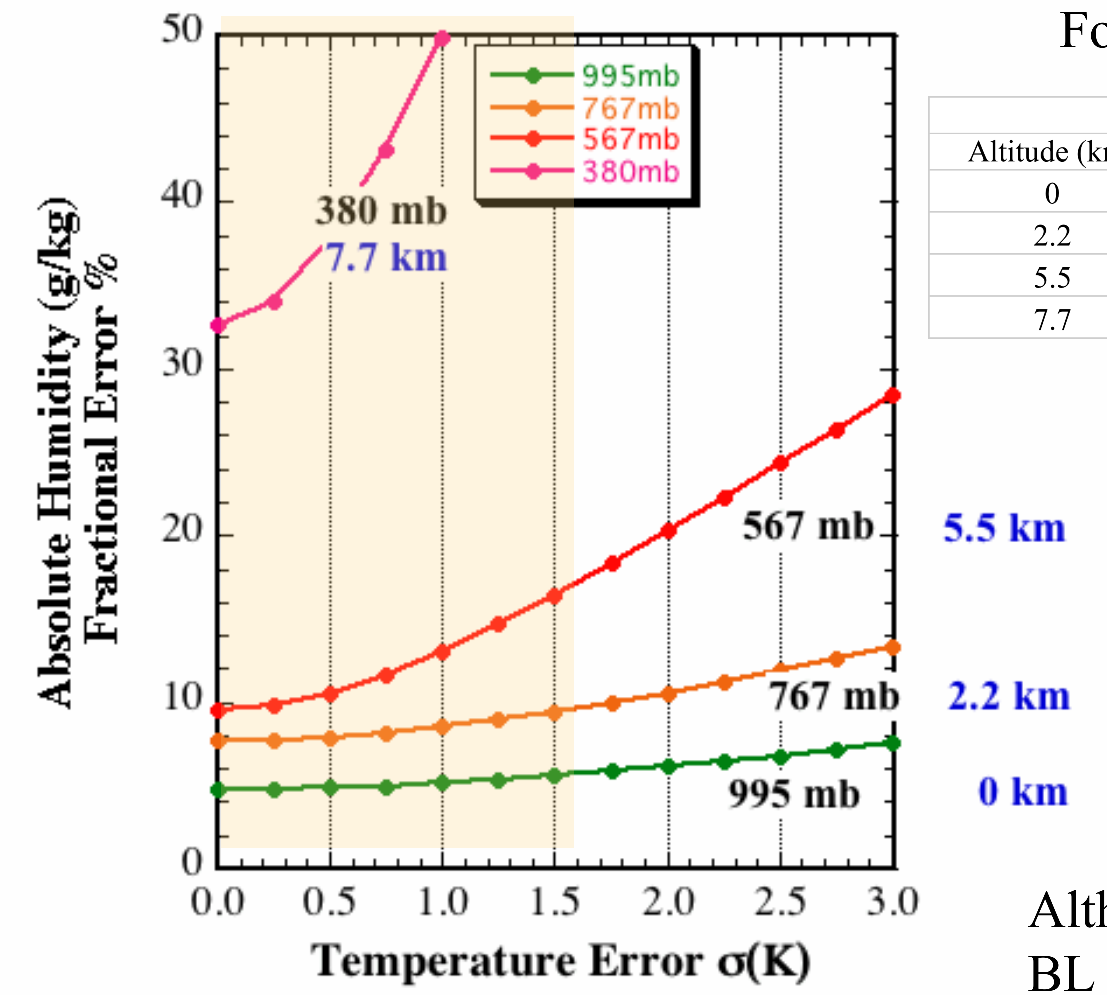

Kursinski et al., *GRL* 1995, *JGR* 2001

For a "typical" tropical sounding:

Altitude (km)	Pressure (mbar)	Error 1 K uncertainty	Error 2 K uncertainty
0	995	5%	6%
2.2	767	8%	9%
5.5	567	12%	20%
7.7	380	50%	-

Although not directly applicable to all BL cases because of temperature inversions – *q dominates refractivity*

Water Vapor Retrievals Lower Troposphere

Assume a temperature from an analysis

Estimated RMS errors for q

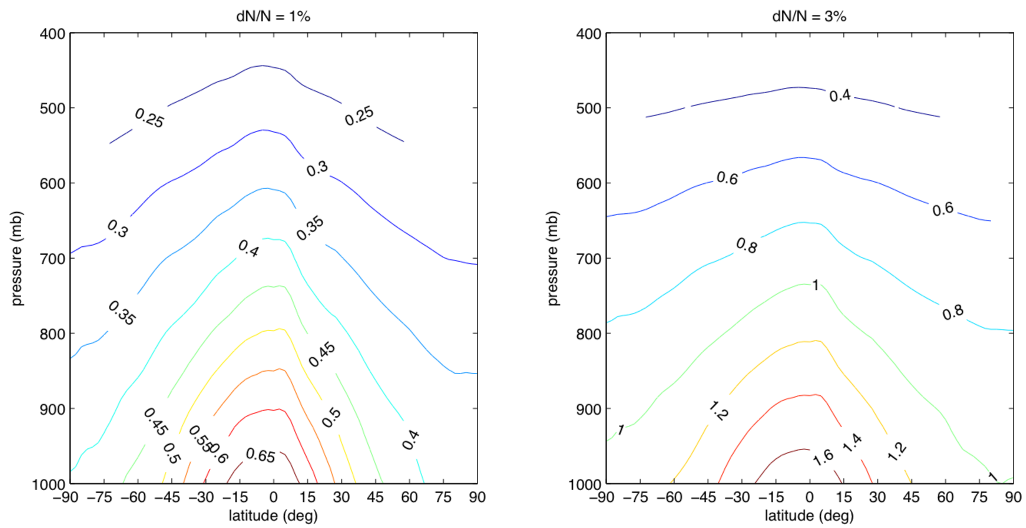

RMS diff. in N and q wrt RAOB

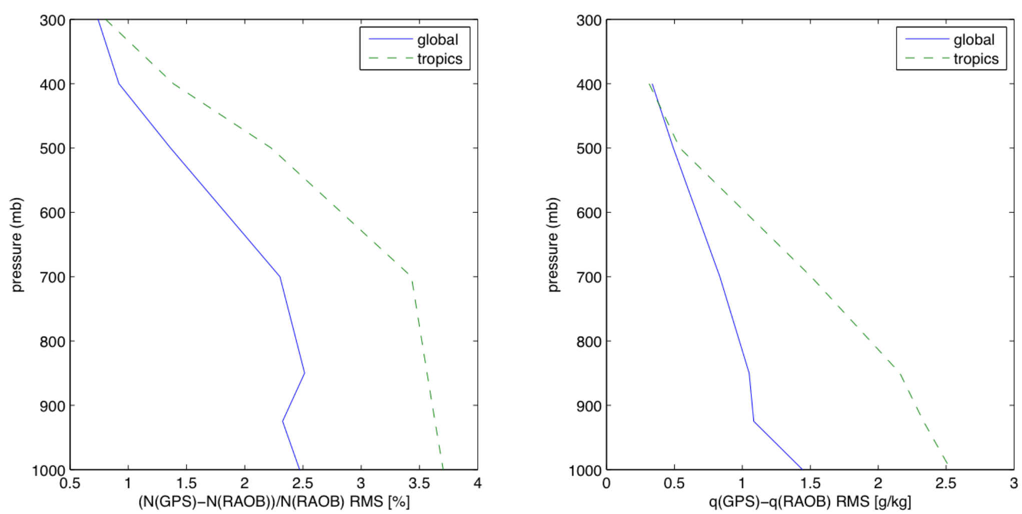

Recent Results

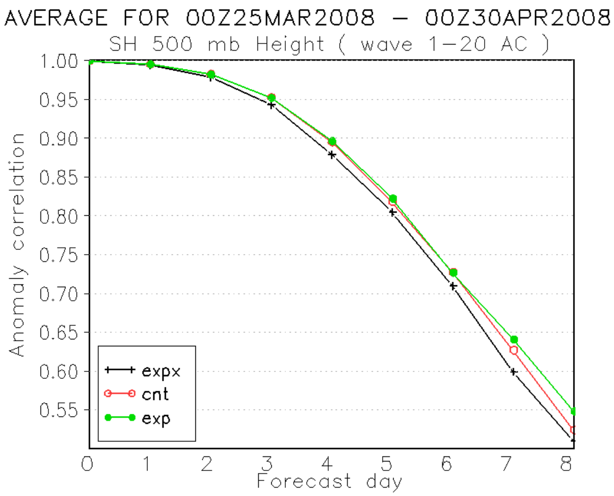

COSMIC provides 8 hours of gain in forecast skill starting at day 4

Details:

- Anomaly correlation scores (the higher the better) as a function of the forecast day for the 500 mb gph in Southern Hemisphere
- 40-day experiments:
  - expx (NO COSMIC)
  - cnt (old RO assimilation code - with COSMIC)
  - exp (updated RO assimilation code - with COSMIC)

The Polar Summer Tropopause Inversion Layer

From Randel and Wu, submitted to *Journal Of The Atmospheric Sciences*

GPS profiles show excellent agreement with *high resolution* radiosondes, capturing the inversion layer

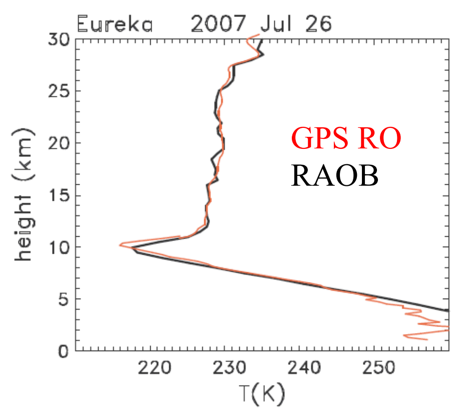

Many more COSMIC observations than high-resolution radiosondes (COSMIC: ~5,000 profiles per month poleward of 60°)

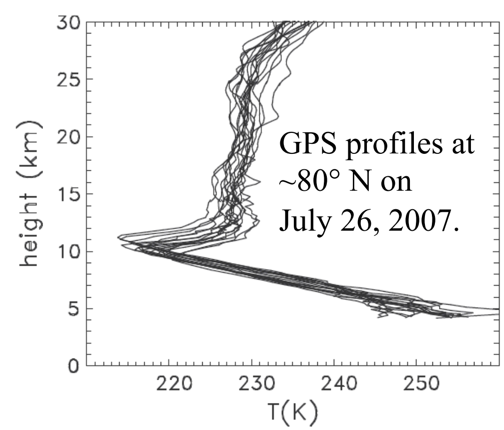

ECMWF Results

SH 100 hPa radiosonde temperature first-guess/analysis error statistics
2001 onwards CHAMP (150), 2006 onwards COSMIC (2000)

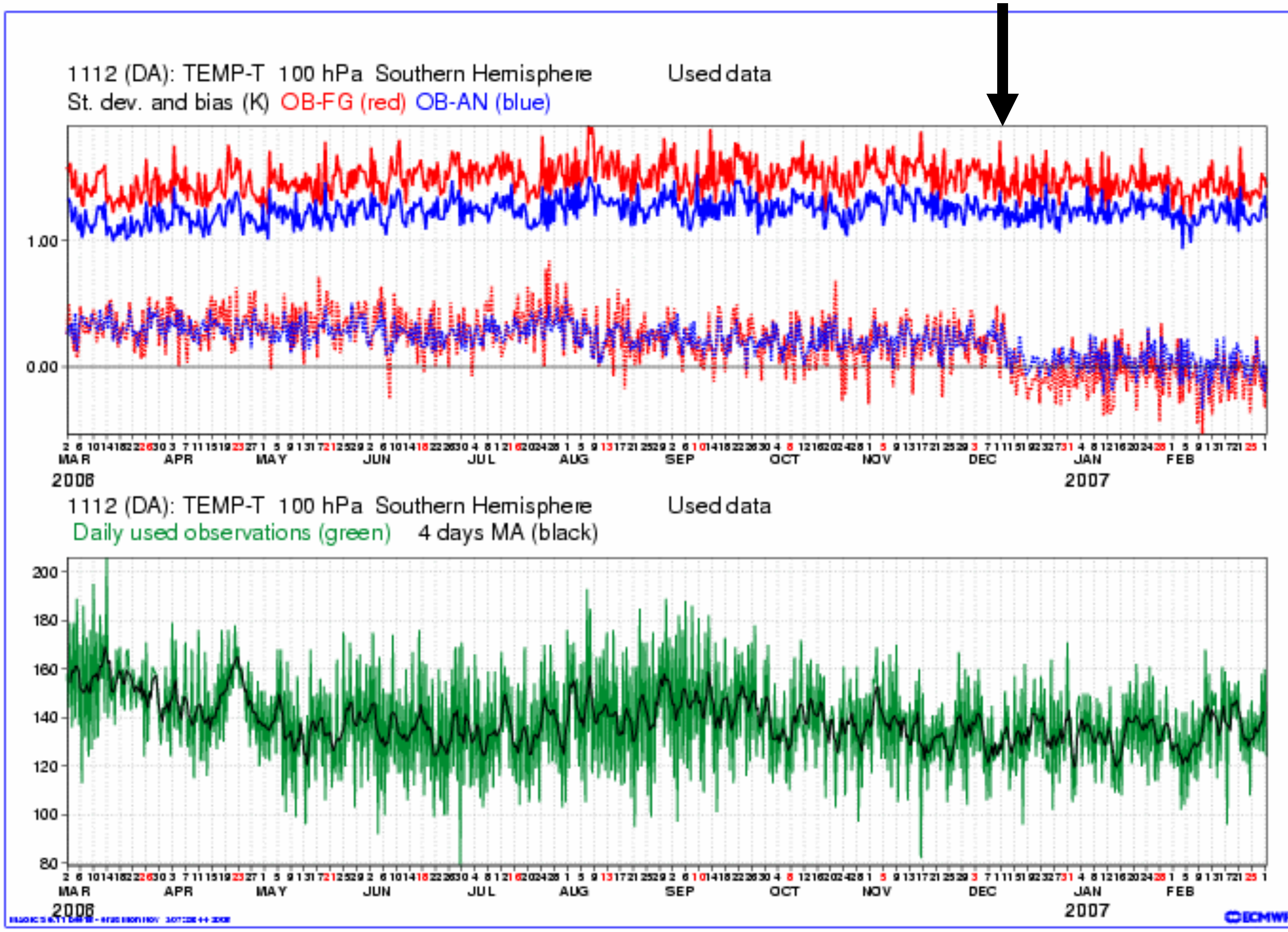

(S. Healy)

ECMWF: Impact On Radiance Biases

Anchoring of radiance bias correction with GPSRO observations:

Metop AMSU-A channel 9 departure & bias correction evolution

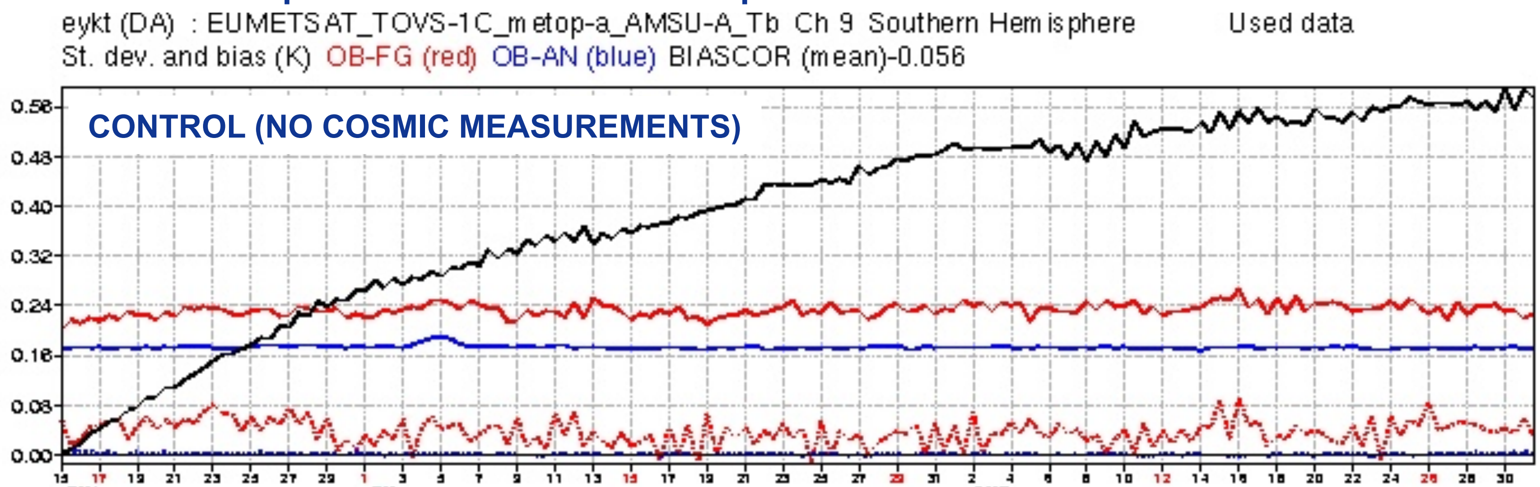

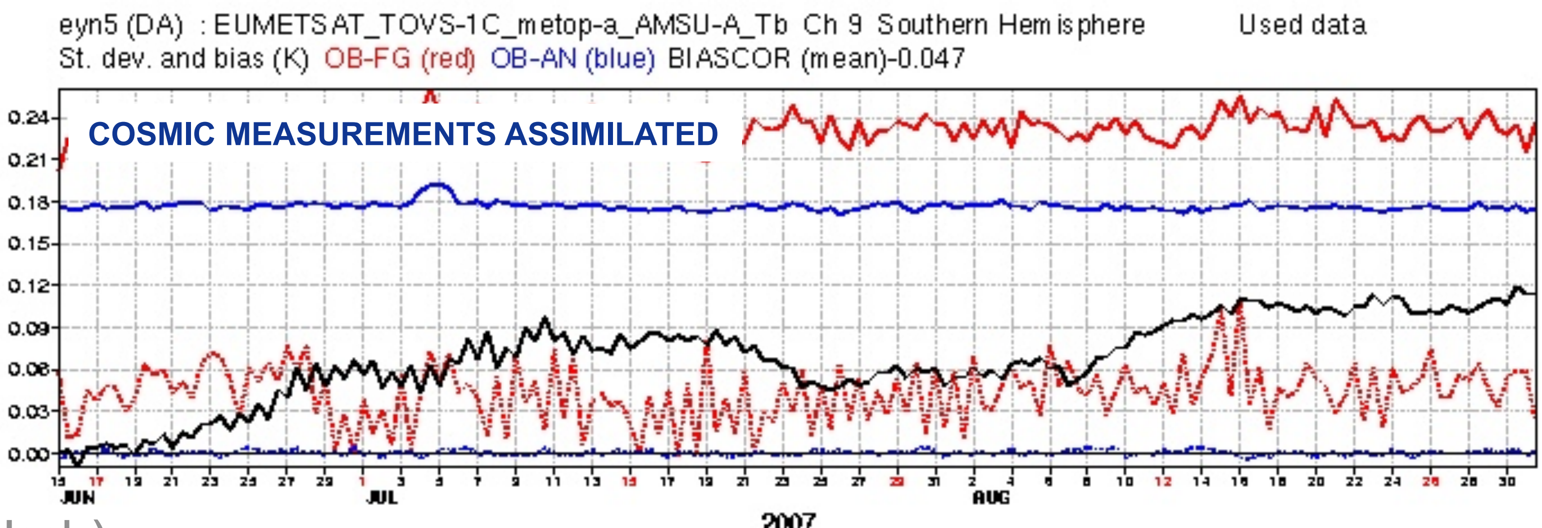

(S. Healy)

RO in the Cloudy Boundary Layer

Useful

- **Cloud penetration**
- **Sensitivity to water *vapor***
  - **Wet term tends to dominate refractivity gradients in ABL**
- **Insensitive to liquid water and aerosol (complementary)**
- **High vertical resolution (50m-200m)**

Less useful

- **Limb measurement – horizontal averaging**
  - **Answer: combine RO with nadir-facing sensors**
- **Current technology: not all soundings reach the surface**
  - **Answer: increase antenna size, fly new receiver "TriG", higher data rates and multiple delay processing**

Boundary Layer Applications

NOTE: BL sensing requirements not levied on RO instruments for current constellations

Definition(s) of ABL heights

How to compute the ABL height from GPS RO?

- **Local gradient methods**
  - **Minimum gradient of refractivity profile [Sokolovskiy et al. 2006; Basha and Ratnam 2009]**
  - **Minimum gradient of specific humidity profile [Ao et al. 2008]**
- **Bulk moisture method:** ***q(pblh) = ½ q(surf)***

Seidel et al.: on comparative study of several ABL height definitions with *radiosonde* data shows that gradient based heights can be very different from traditional mixing heights.

Seidel, Ao and Li, *JGR* 2010

Defining the ABL Top

- ***Local Gradient*: Define ABL top as height where *dq/dz* is minimum**

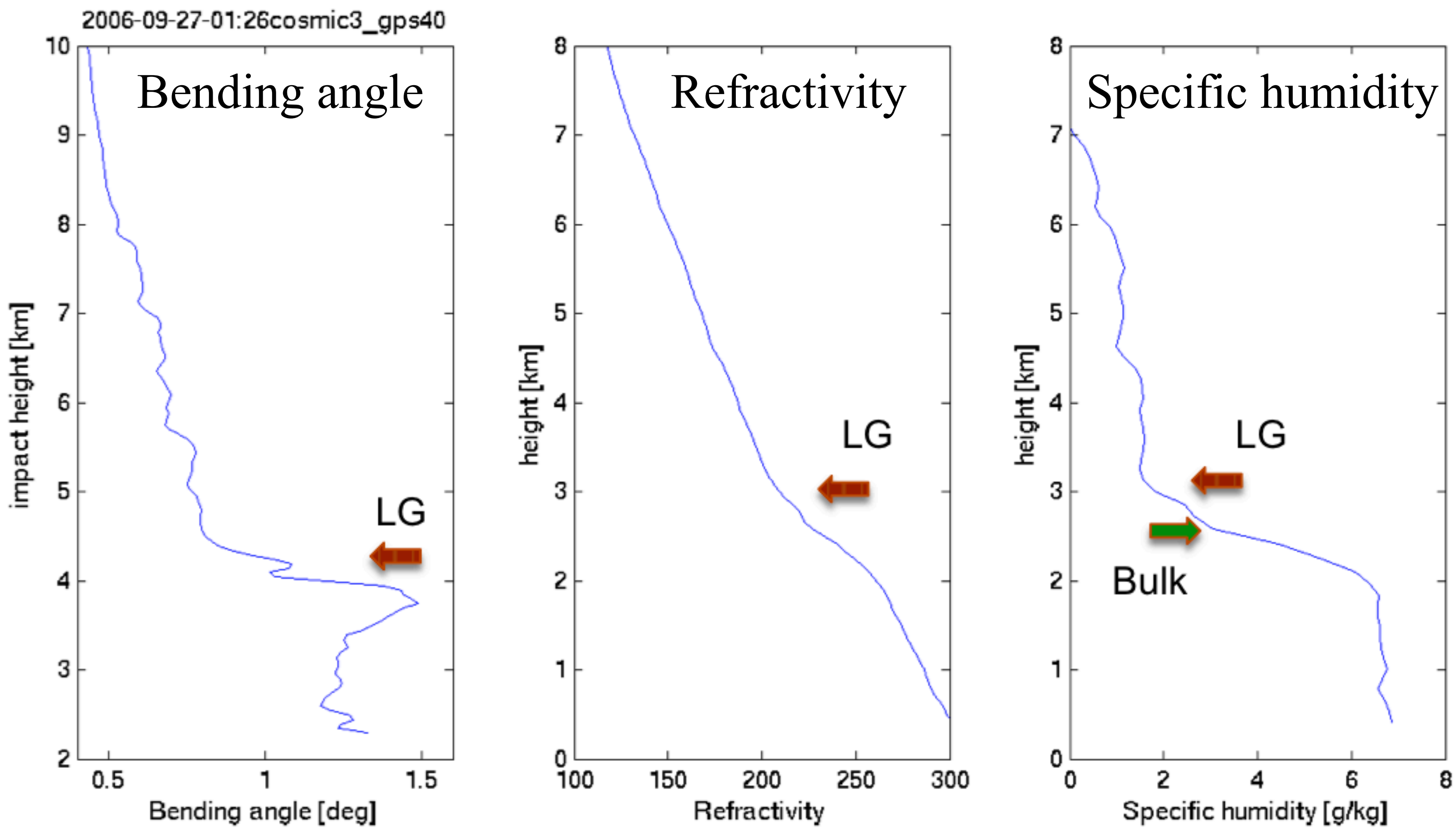

- ***Bulk Moisture***: Define ABL top as height where $q = ½\ q(surf)$

Comparison with RAOB/Hi-Res

dq/dz method

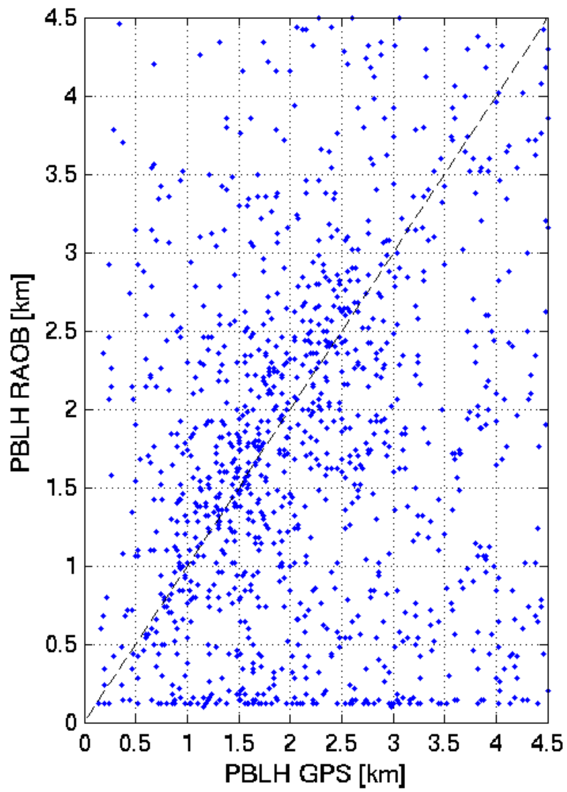

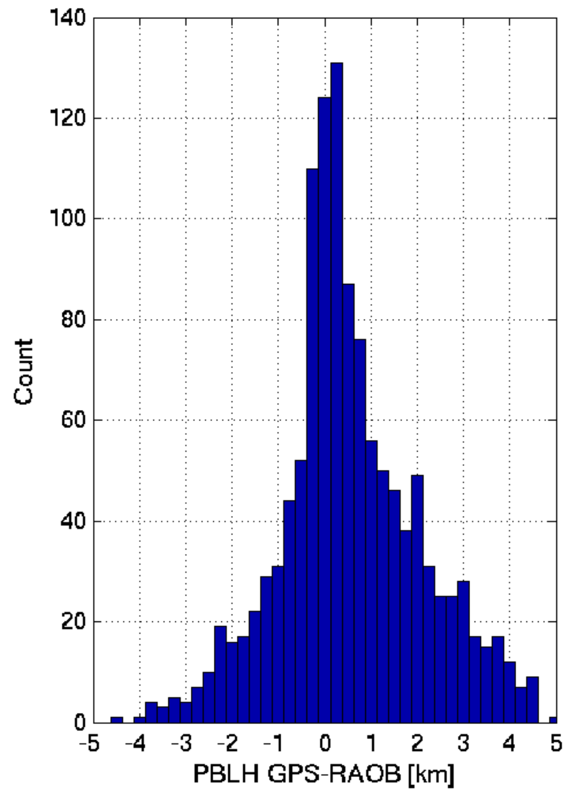

All profiles < 300 km, 3 hr apart

- Restrict comparisons to profiles with min alt < 0.5 km above surface
- Exclude the lowest 200 m of both GPS and RAOB profiles

➡ Need improved technology for RO to consistently reach surface

Minimum Profile Depth

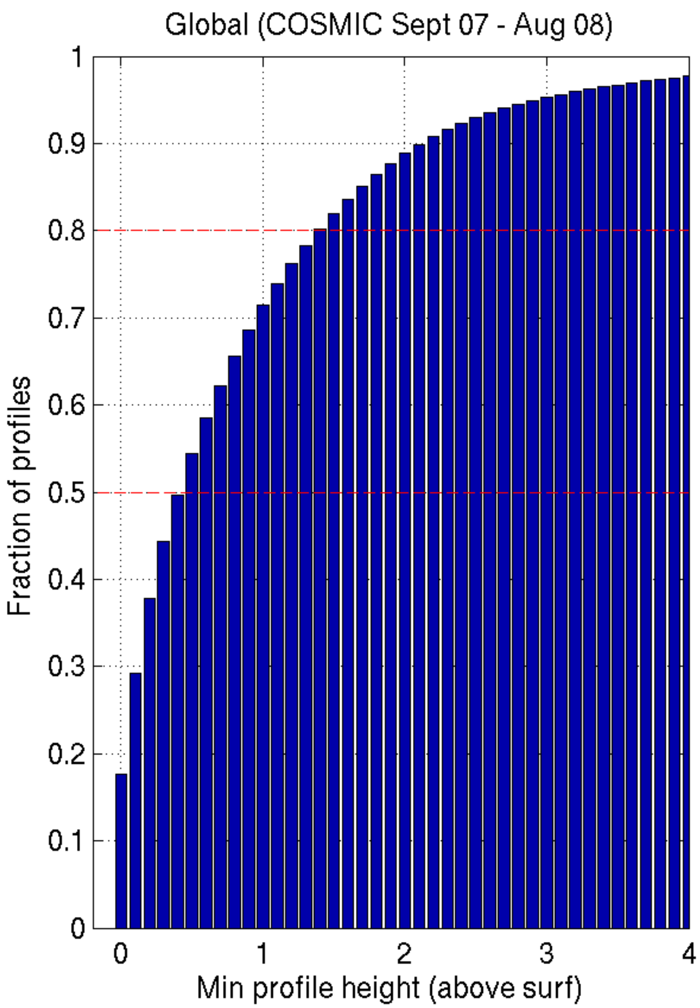

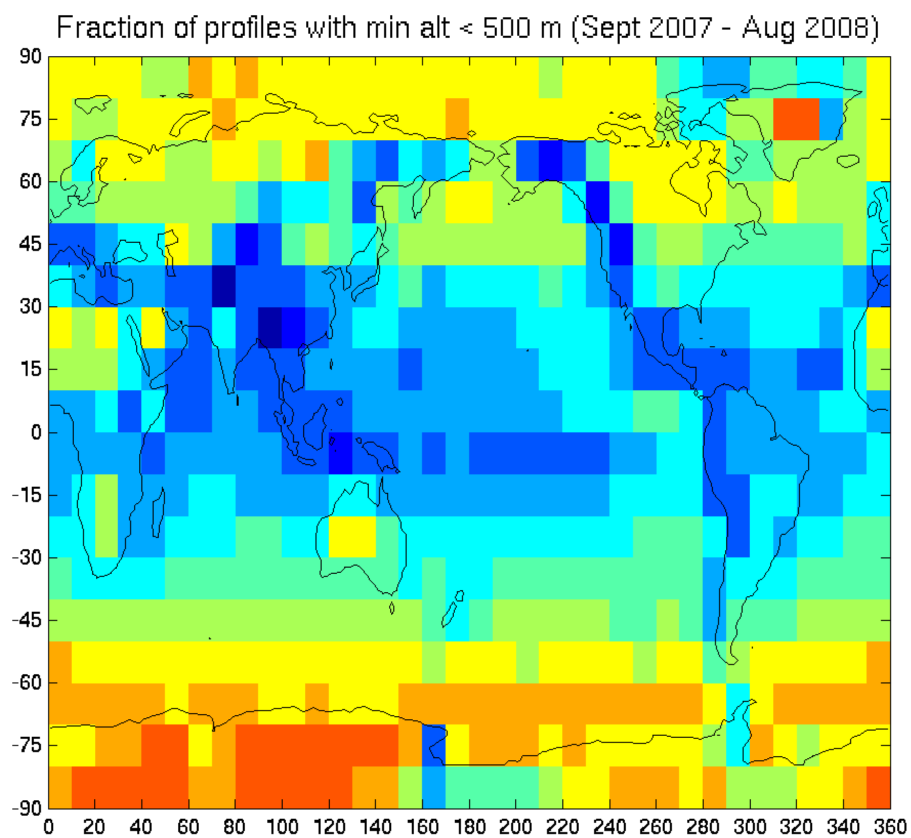

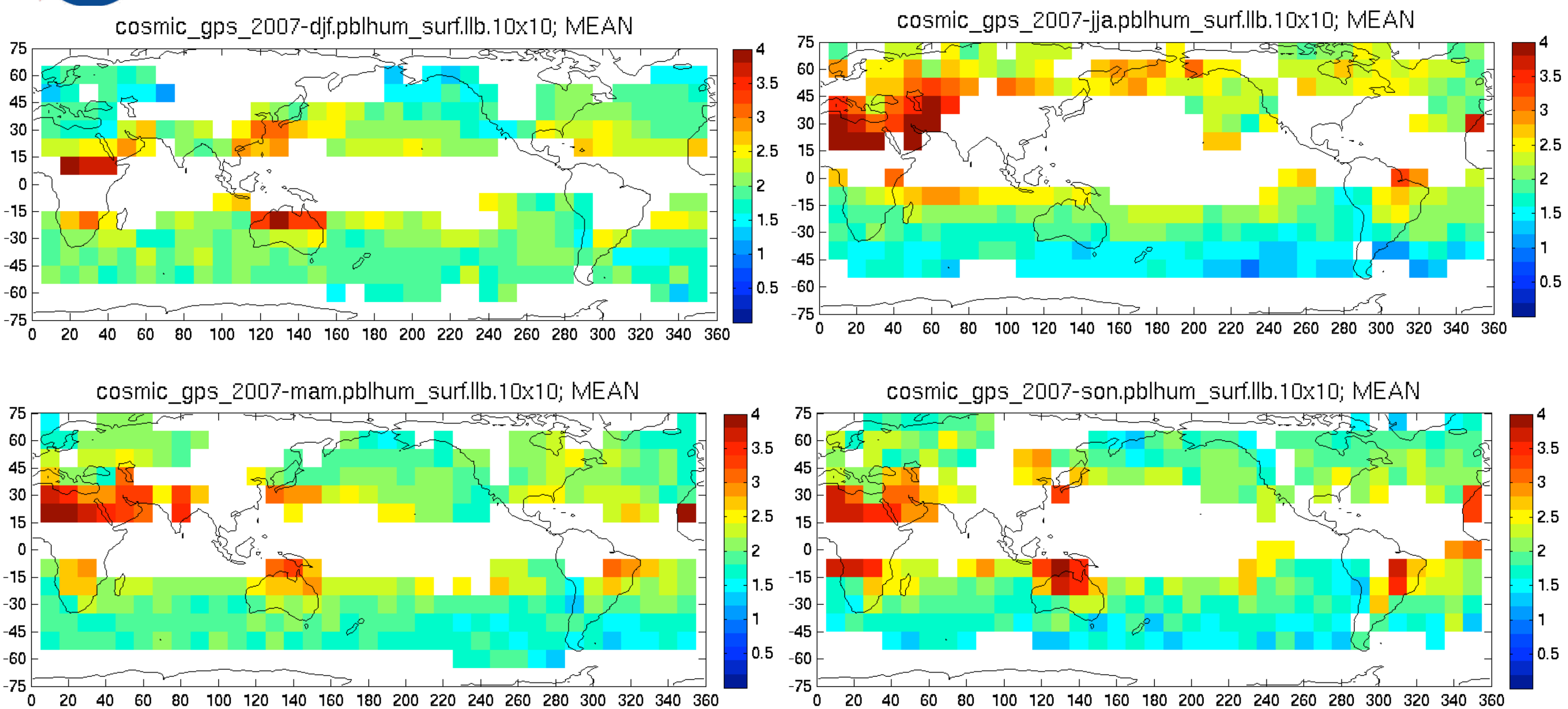

cosmic 2007 data, 10x10 grids, seasonal averages

minimum dq/dz, no smoothing,
only include sharp profiles, defined as dq/dz < -5 g/kg/km and (dq/dz)/median(dq/dz) > 10

"Sharp" PBL Tops

Distribution of top 25 %-tile in humidity gradients at PBL height

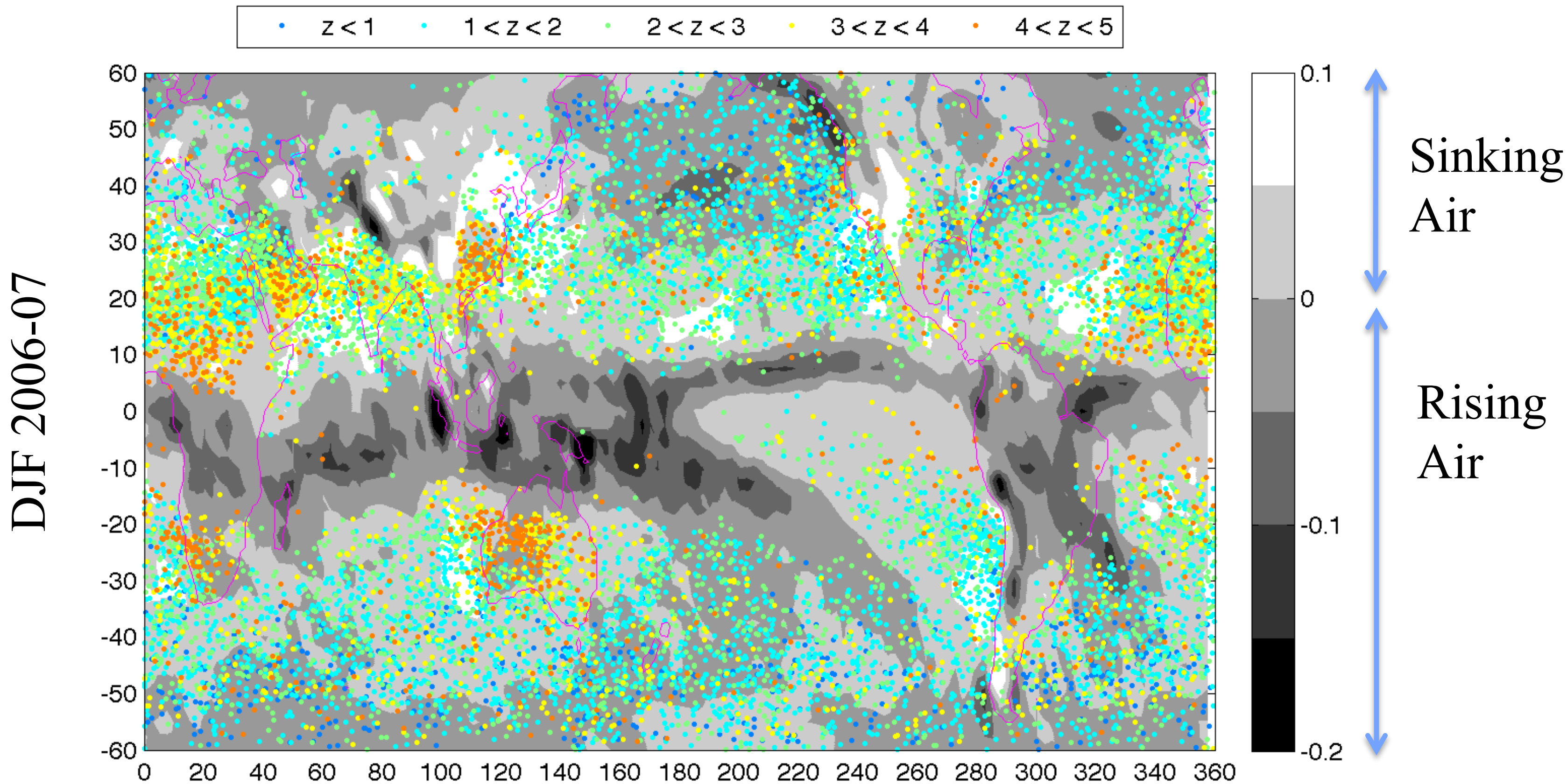

Vertical velocity from ERA-40 500 hPa (2000-2001)

January 2007

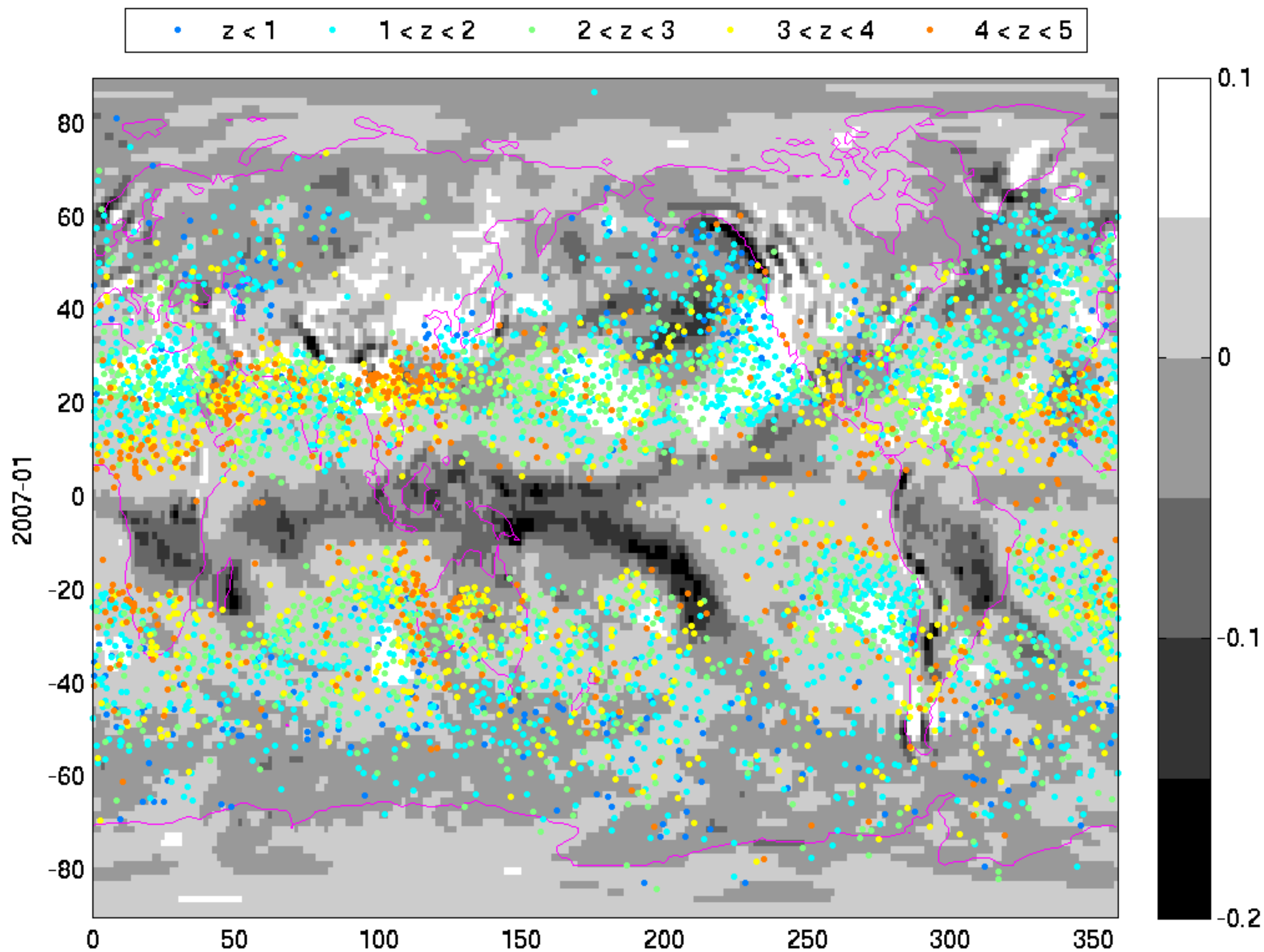

ERA-Interim

August 2007

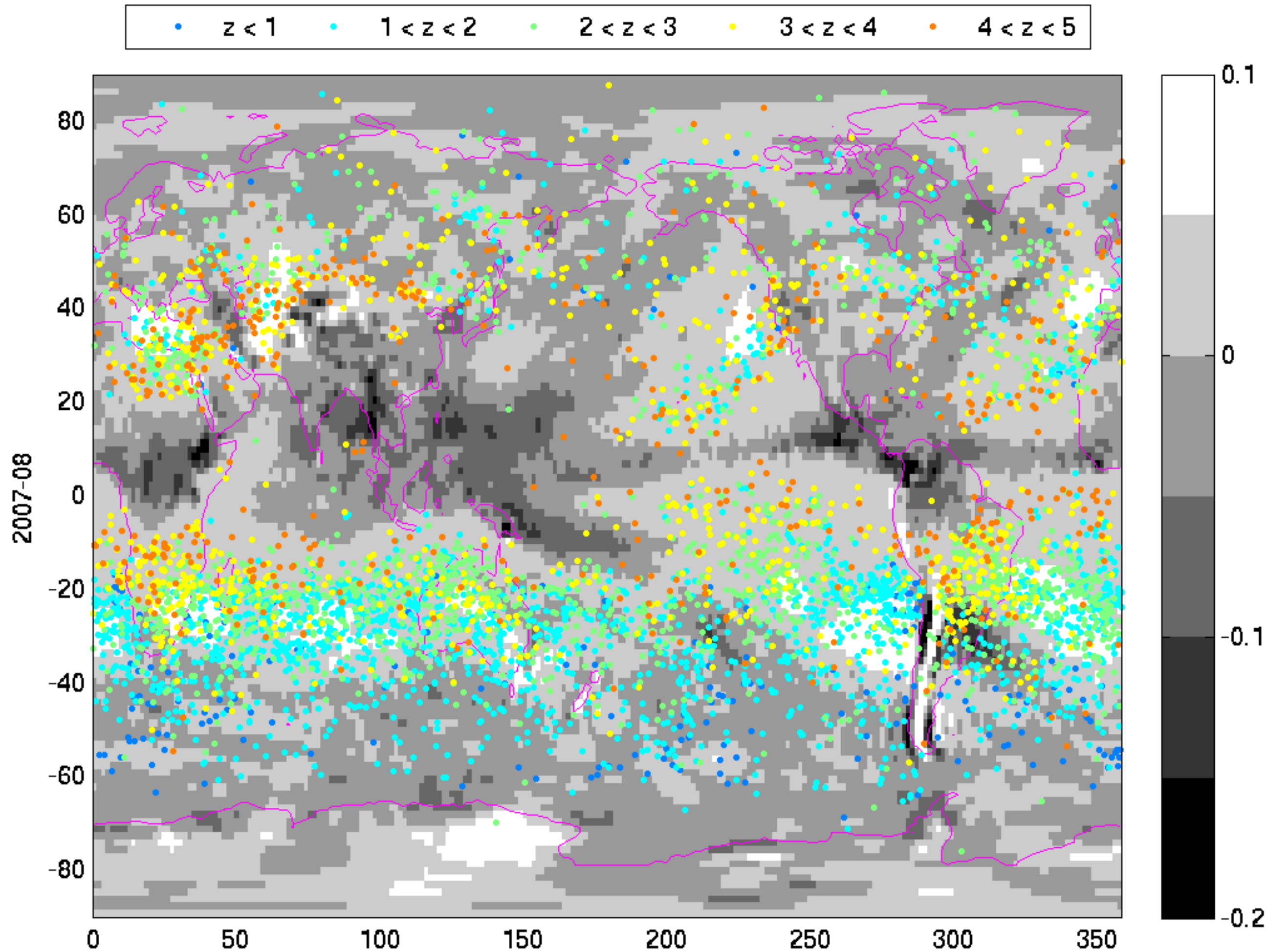

ERA-Interim

COSMIC – 3 years of data

Based on bending angle lapse rate

Diurnal variations of the ABL depth

(thin lines – standard deviations of the mean)

North Pacific

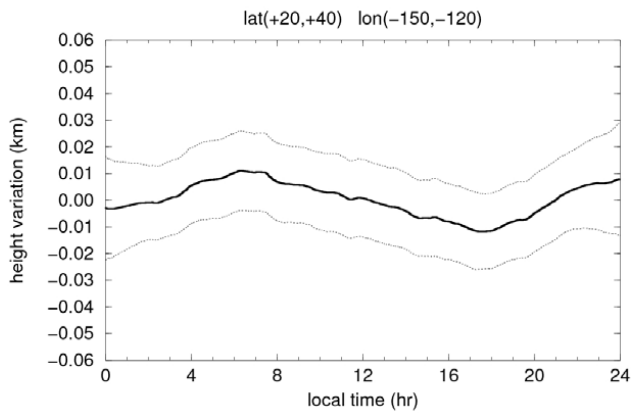

South Atlantic

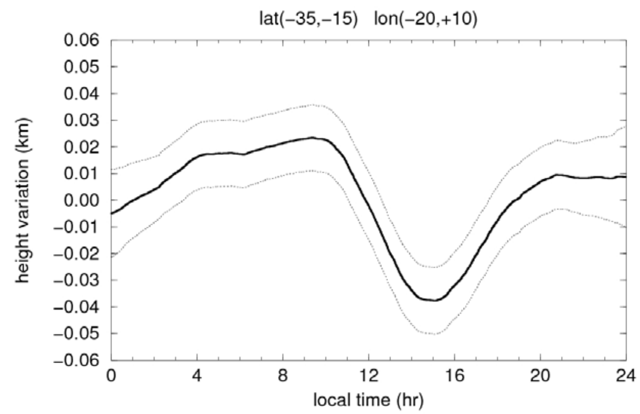

South Pacific (I)

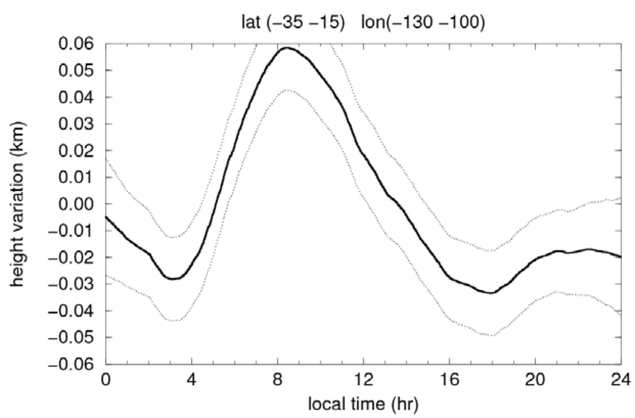

South Pacific (II)

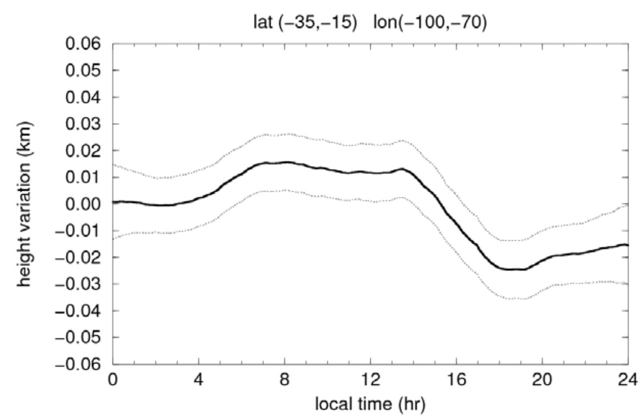

Sokolovskiy et al., AMS Annual Meeting 2010

COSMIC (cont.)

Validation of the diurnal variations of the ABL depth with atmospheric models is difficult because the models:
(i) do not provide sufficient vertical resolution at the ABL top
(ii) do not provide uniform sampling in local time

Internal validation: estimation of the diurnal variation over desert produces expected results (deeper ABL in the afternoon).

Sahara Desert

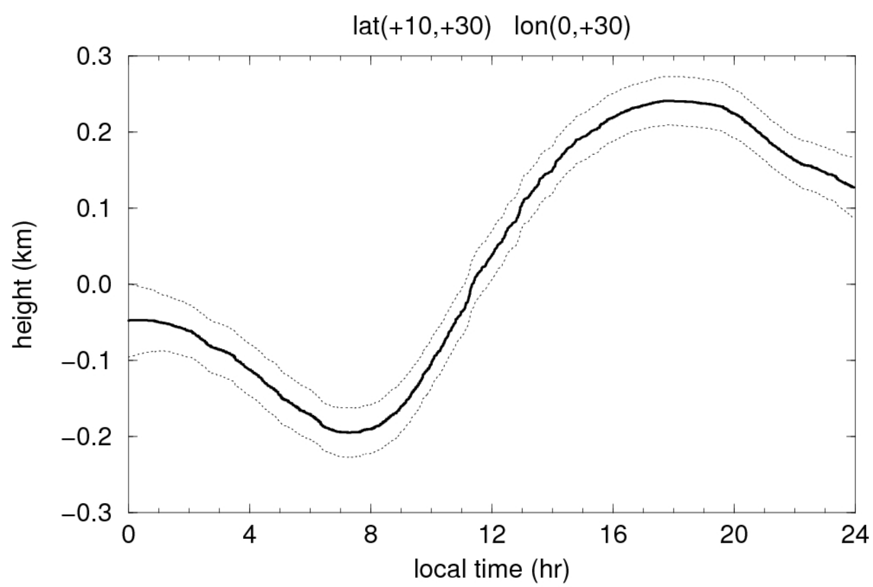

Sokolovskiy et al., AMS Annual Meeting 2010

Case Study: Lihue, Hawaii

Xie et al., GRL 2010

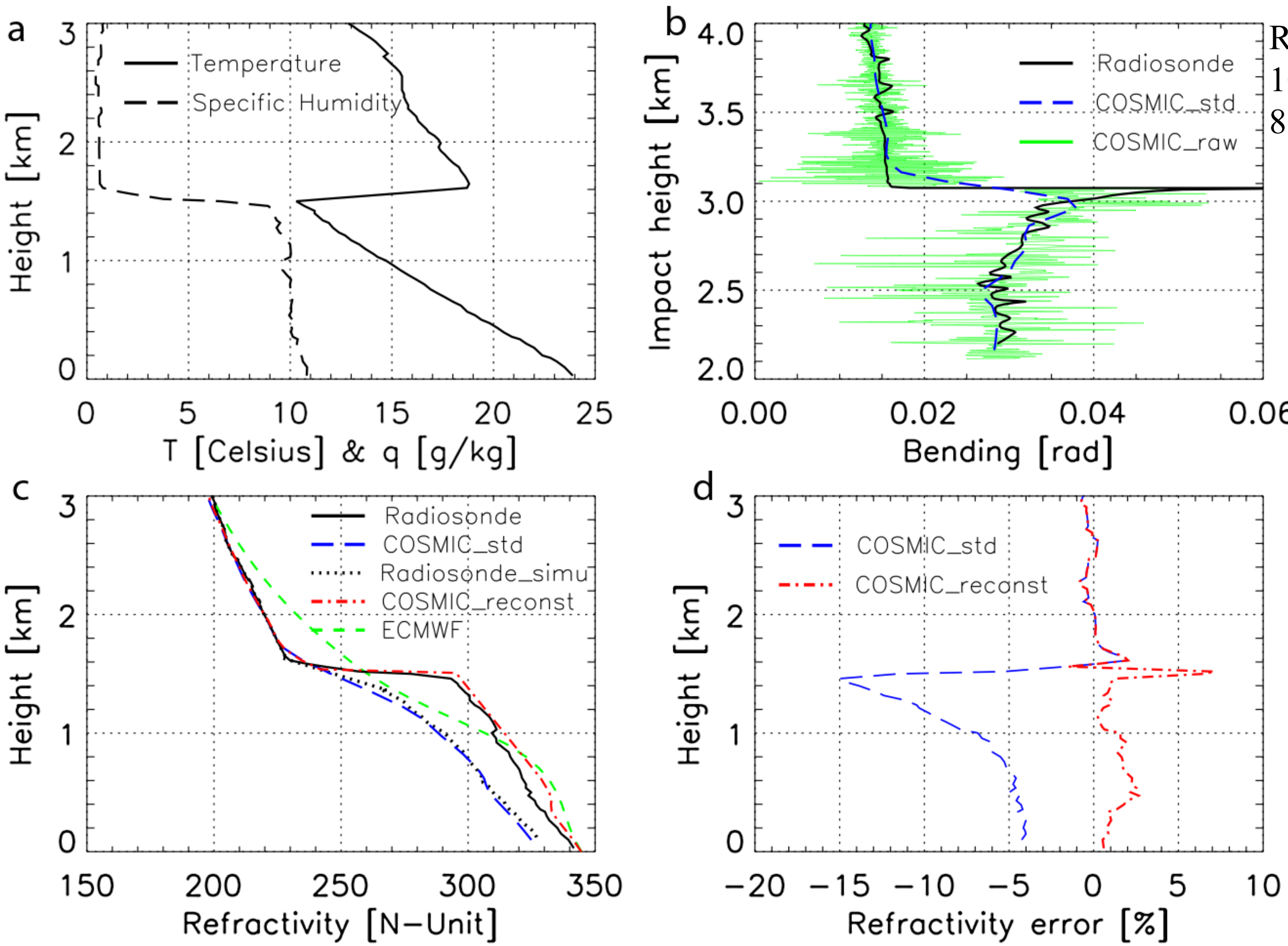

RO-RAOB
10 min
85 km

RO Remote Sensing in Context

- **Passive (AIRS, MISR, …)**
  - **A natural source provides the photons**
    - Often this creates possibility to form a 2D image
  - **Radiative transfer**
    - Count photons of a specific frequency or spectral band
- **Active backscatter (Radar, LIDAR, …)**
  - **Sensitive to particulates, scatterers**
  - **Range gating and discrimination of different scatterers**
- **Active transmission (RO with GPS or other sources)**
  - **Phase shifts sensitive to atmospheric density and water vapor**
  - **Interferometric: received signal is coherent superposition of phase shifts along the beam and vertically**

The Forward Problem in RO

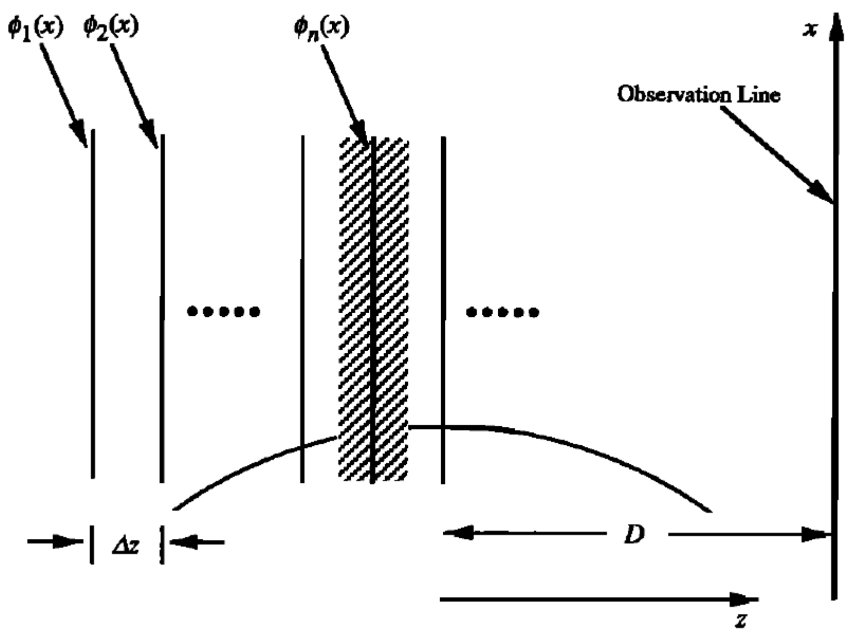

Scalar diffraction theory, polarization effects ignored at L-band

Source of phase shift

$$\phi_n(x) = k \int_{z_n - \Delta z/2}^{z_n + \Delta z/2} [\mu(x, z) - 1]\, dz$$

Impact of phase shift

$$u(x, z_n^+) = u(x, z_n^-) \exp[i\phi_n(x)]$$

Decomposition into plane waves

$$U(k_x, z_n^+) = \int_{-\infty}^{\infty} u(x, z_n^+) e^{-ik_x x}\, dx$$

Free space propagation

$$U(k_x, z_{n+1}^-) = U(k_x, z_n^+) \exp(ik_z \Delta z)$$

Signal reconstruction

$$u(x, z_{n+1}^-) = \frac{1}{2\pi} \int_{-\infty}^{\infty} U(k_x, z_{n+1}^-) e^{ik_x x}\, dk_x$$

Measurement Physics

Wavelength of the radiation	0.19	meters
Synthetic Aperture Size	100,000	radius
Diffraction corrected resolution (vertical)	6-60	6 reflects "ideal"
Distance traveled to shift phase 1/2 wavelength	850	at 2 km altitude

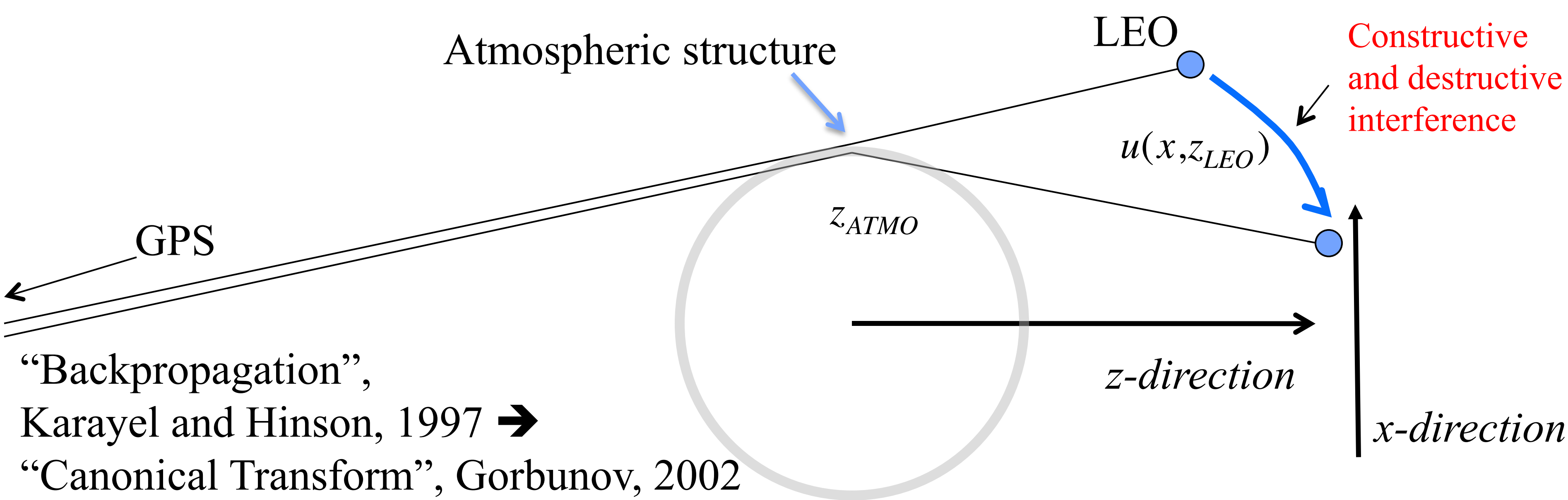

"Backpropagation",
Karayel and Hinson, 1997 ➔
"Canonical Transform", Gorbunov, 2002

Received Signal

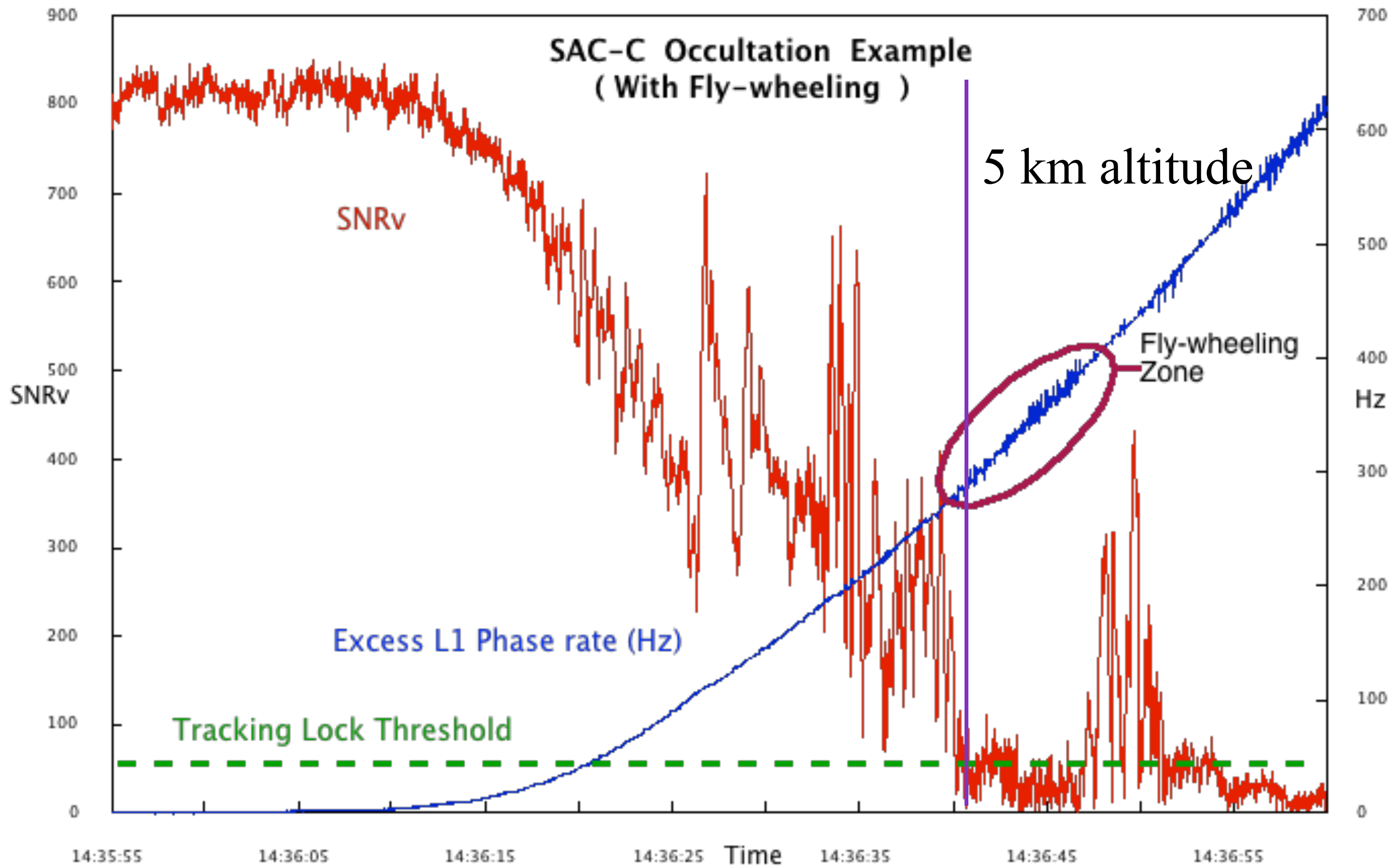

Courtesy of Tom Meehan

Signal Dynamics and Atmospheric Structure

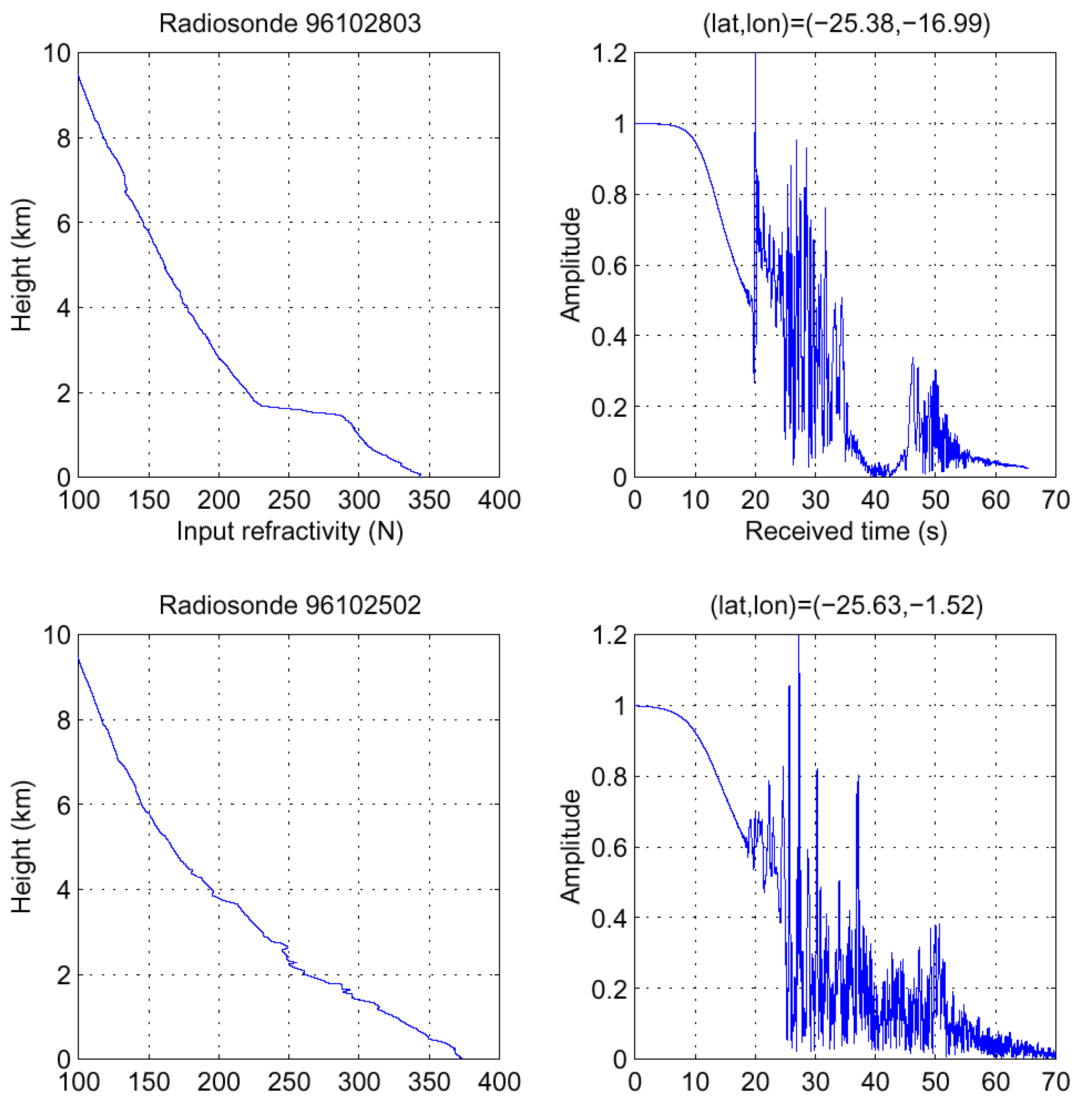

Simulations demonstrate that the received signal is very sensitive to kinks in atmospheric density structure

Recent Results Using Large Eddy Simulations and Mesoscale Models

- **The following results show simulated signal structure after propagation through simulated atmospheric fields with small-scale structure characteristic of BL features of interest**

Acknowledgement: Research and Technology Development (R&TD) program, JPL

Recent Results Using Large Eddy Simulations and Mesoscale Models

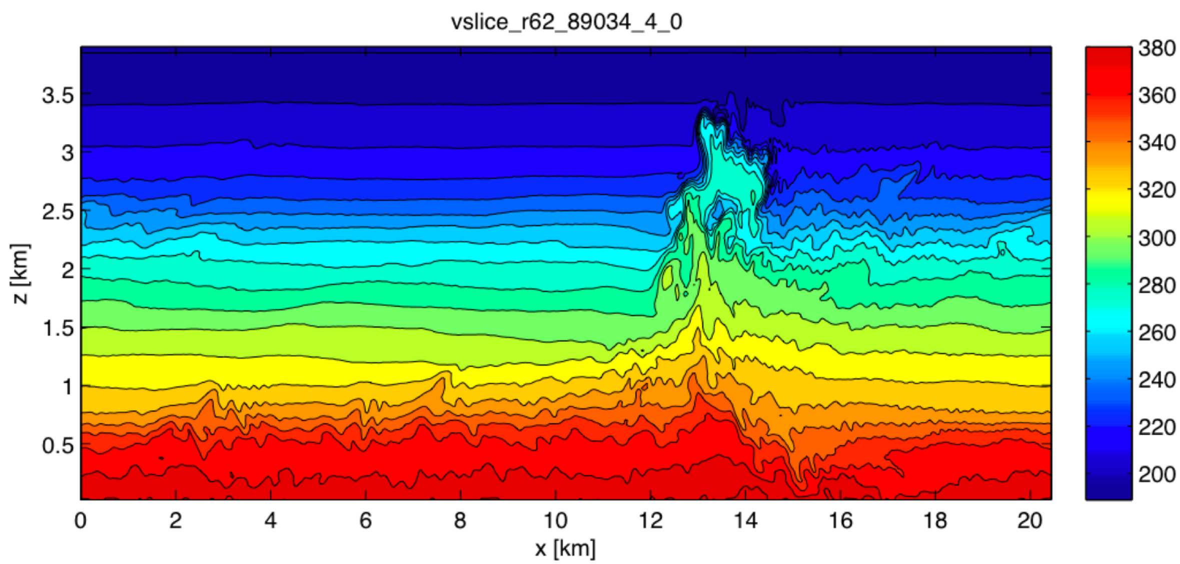

40 m resolution
LES simulation

Refractivity structure within and outside a convective plume

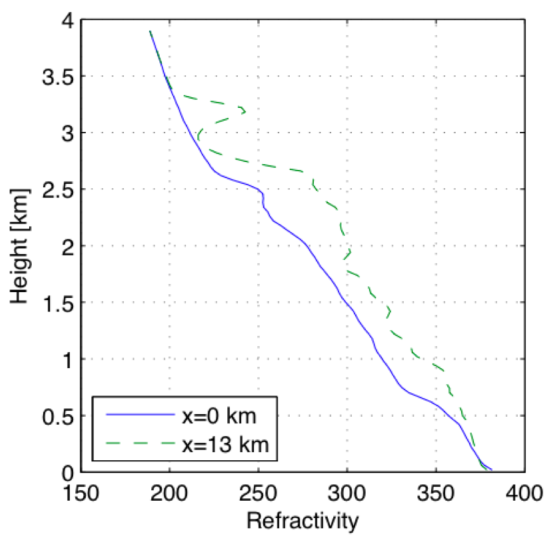

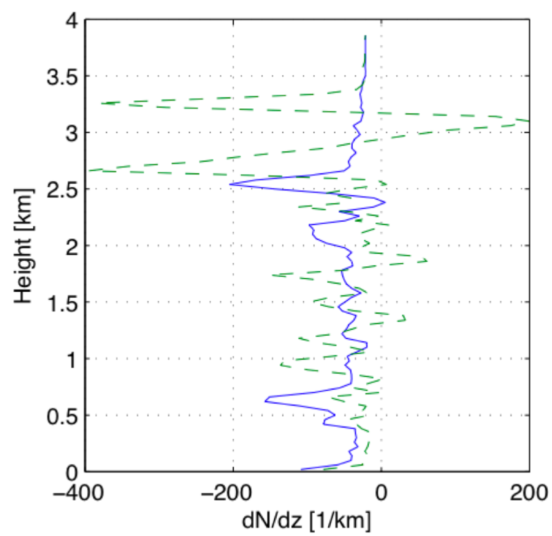

Acknowledgement:
Georgios Matheou, JPL

Simulated Signal Amplitude

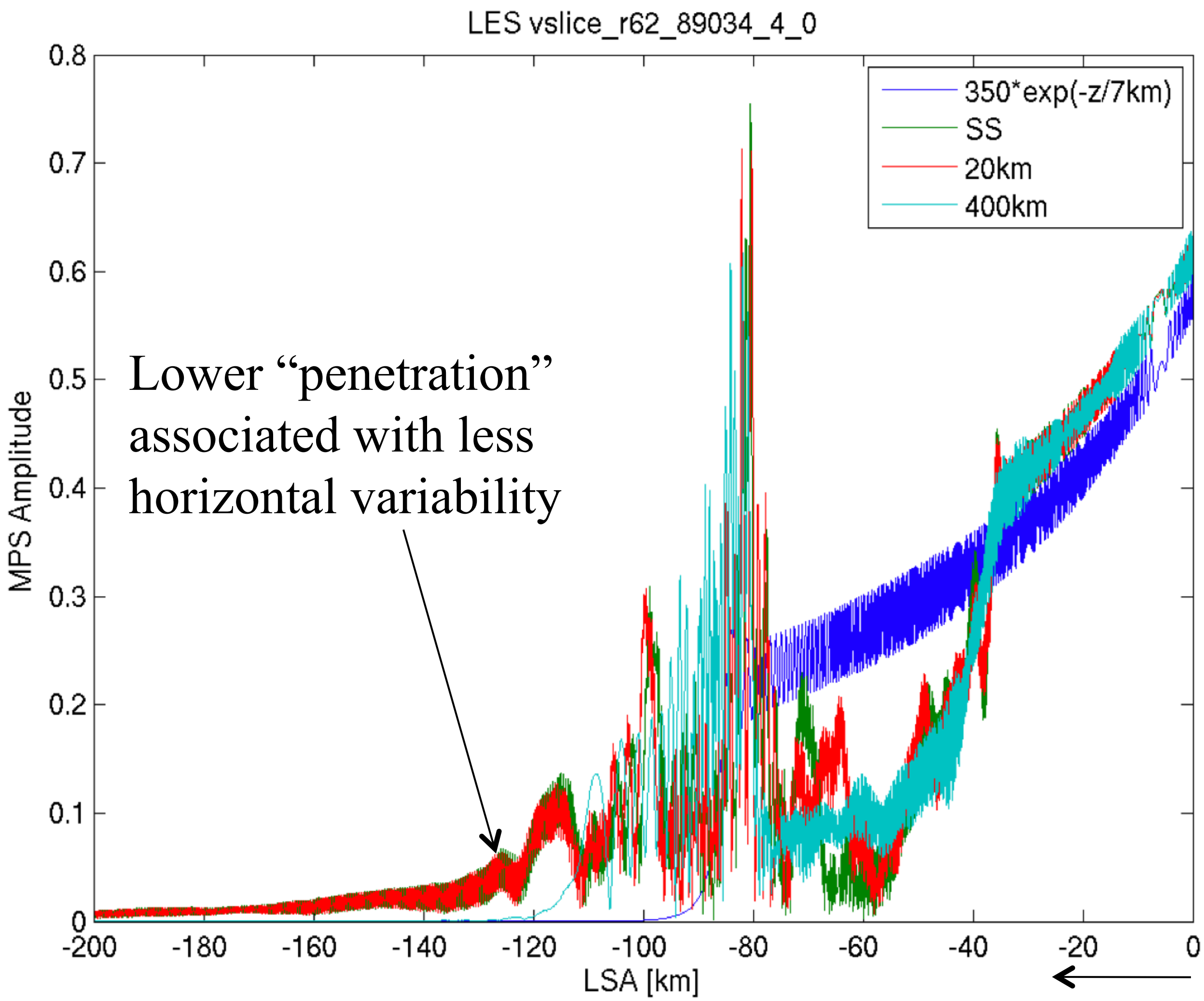

LSA: Measure of vertical coordinate

descending

350: smooth refractivity profile

SS: continue LES structure of x=0

20 km: LES structure embedded in a smoother background

400 km: LES structure repeated (periodic boundary conditions)

20 km and 400 km cases contain convective plume

SS "Spherical symmetry"

Amplitude of the Integral Transform

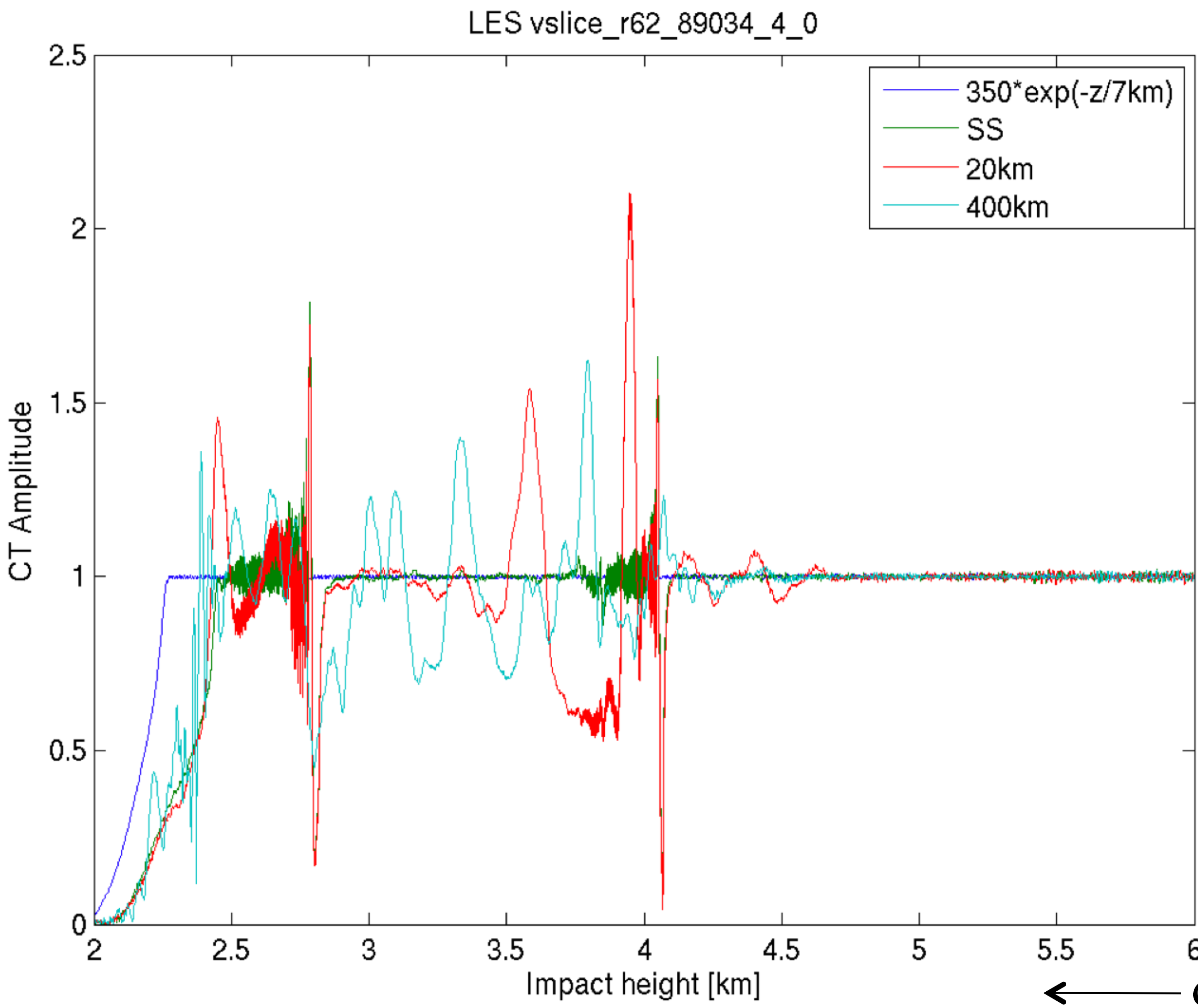

Amplitude of signal decomposed into bending angle/impact parameter space

350: smooth refractivity profile

SS: continue LES structure of x=0

20 km: LES structure embedded in a smoother background

400 km: LES structure repeated (periodic boundary conditions)

20 km and 400 km cases contain convective plume

SS "Spherical symmetry"

← descending

Impact height ≈ altitude + 2 km

Weather Front Using WRF

WRF refractivity structure

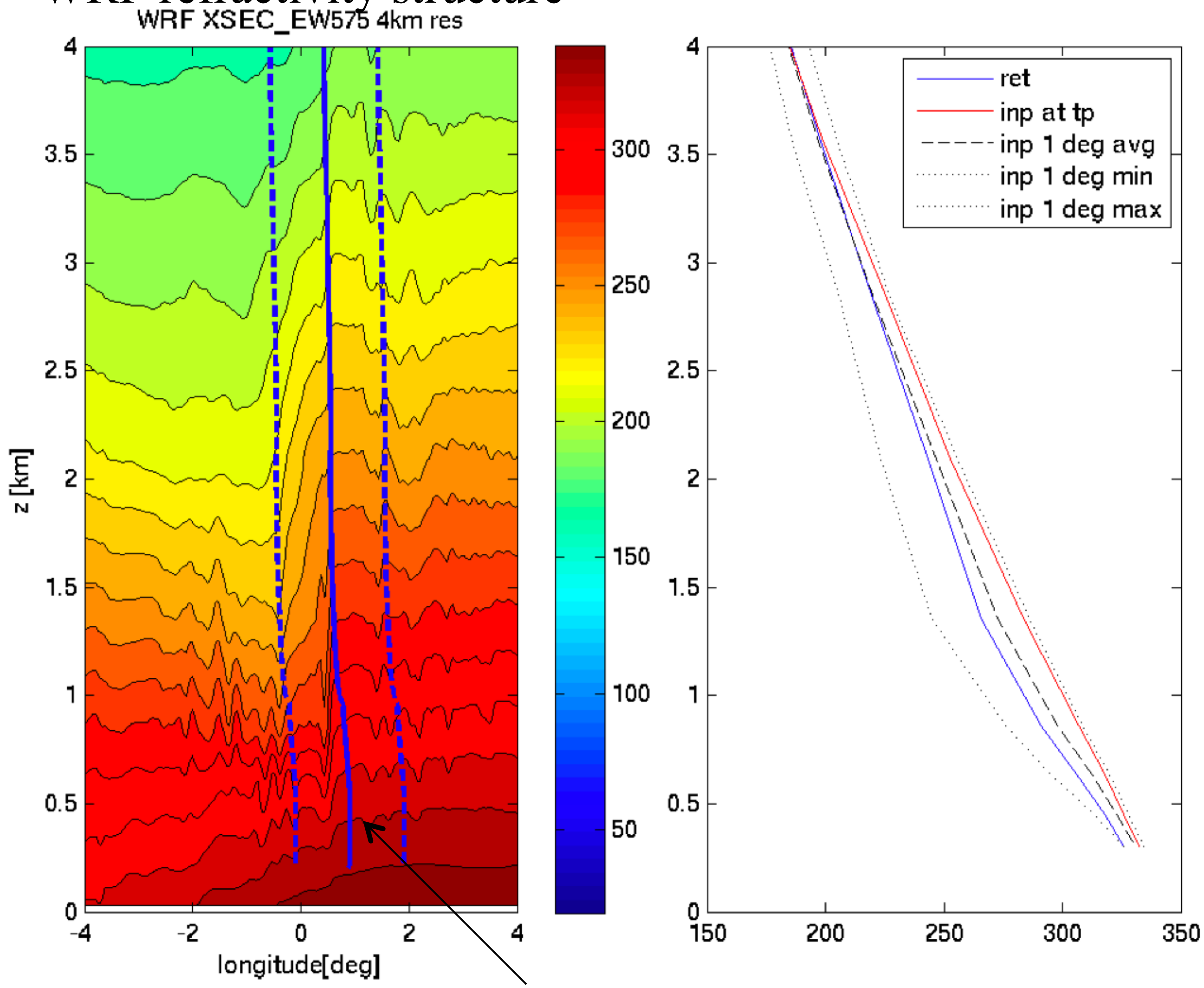

Descending occultation tangent points

ret: retrieved refractivity assuming spherical symmetry

inp at tp: refractivity at tangent point location

inp 1 deg avg: WRF refractivity average within ± 1 degree

inp 1 deg min: WRF refractivity displaced -1 degree from tp

inp 1 deg max: WRF refractivity displaced +1 degree from tp

Acknowledgement:
Svetla Hristova-Veleva, JPL

Case Study: Horizontal Resolution

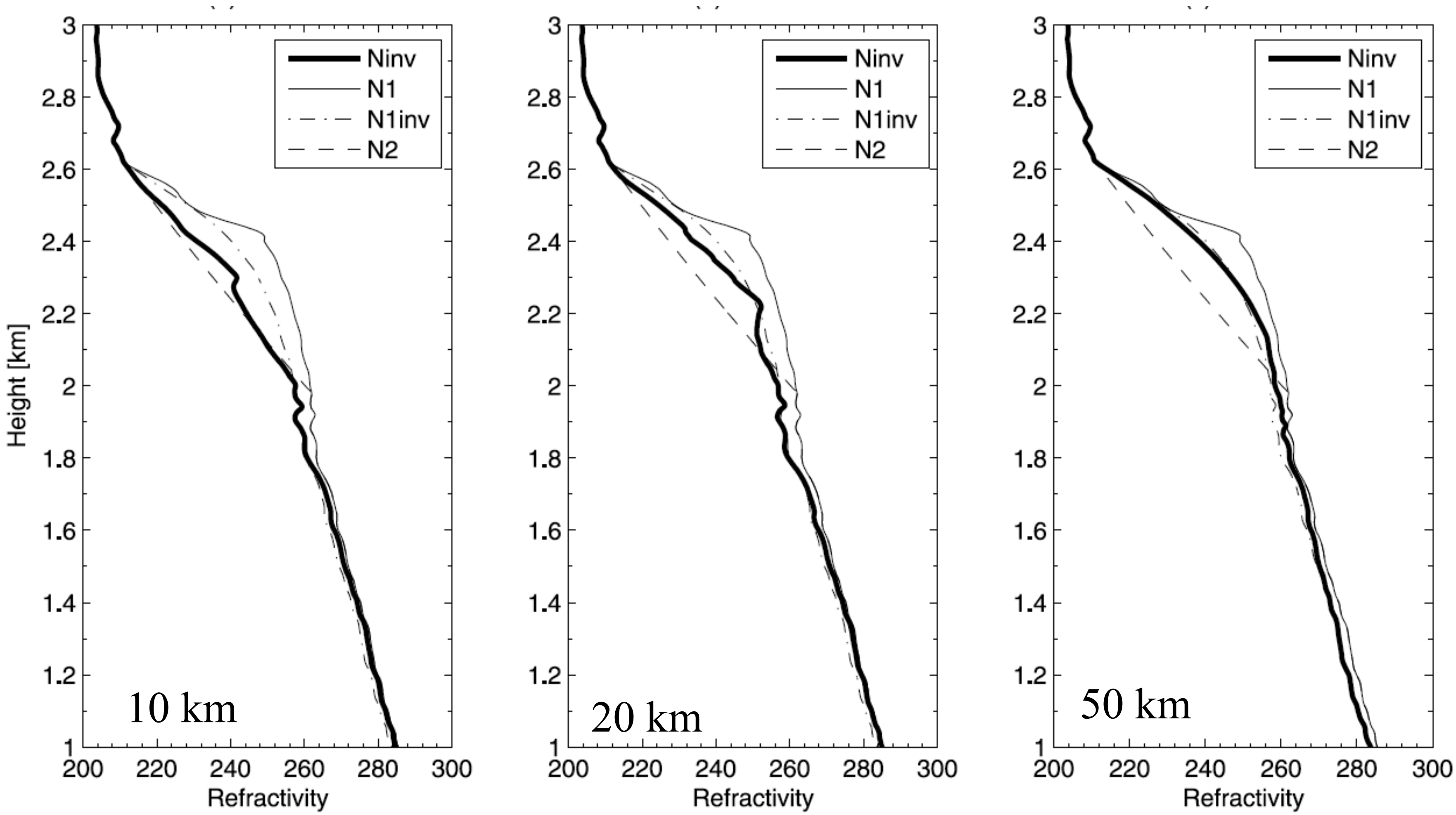

- **50 m vertical retrieval resolution ⇒50 km horiz resolution**

Ao, C. O. (2007), Effect of ducting on radio occultation measurements: An assessment based on high-resolution radiosonde soundings, Radio Sci., 42, RS2008, doi:10.1029/2006RS003485.

RO as a Tool for BL Remote Sensing

- **Science objective: thermodynamic conditions and water vapor within and above the boundary layer. This provides a constraint on the processes that result in the distribution of hydrometeors**
- **Develop new retrieval techniques that:**
  - **Increase use of information in the signal**
  - **Can be combined with other sensors that detect liquid water, ice, etc.**
- **New retrieval methods will (*perhaps*):**
  - **Use a forward model that includes diffraction effects**
  - **Use *a priori* atmospheric information in some form**
  - **Use information from complementary sensor systems**
  - **Account for refractive index variations along the raypath**

Vision

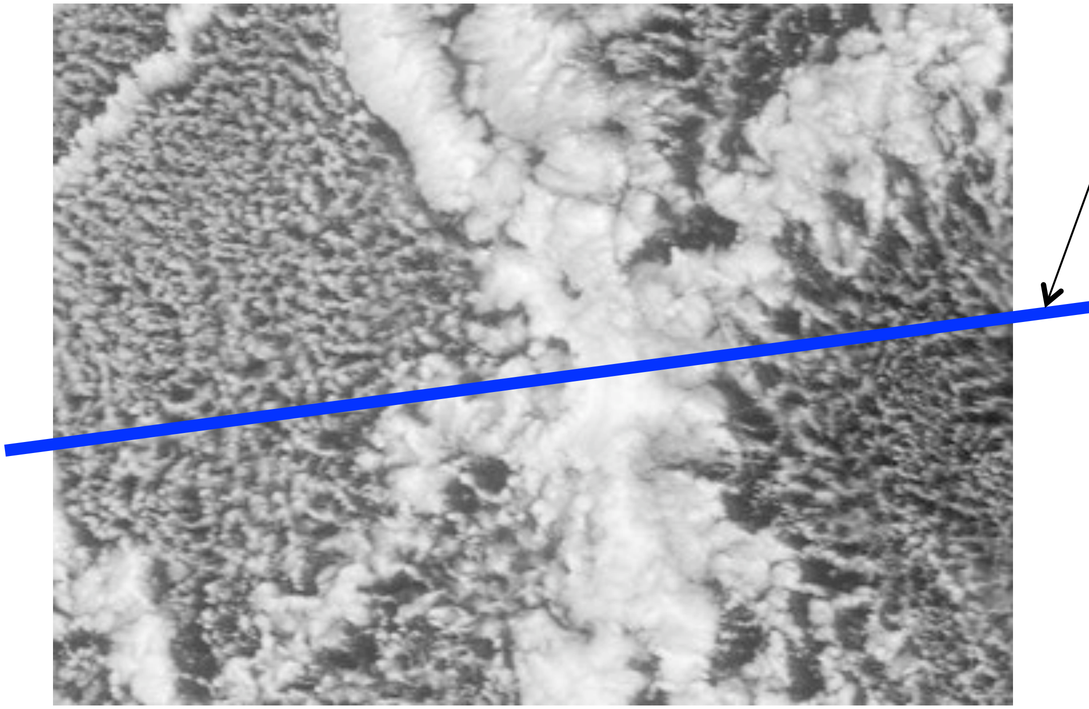

Radio occultation link penetrating this structure, providing information on the thermodynamic and water vapor vertical structure

Accurate forward modeling and the sensitivity of RO provide a very strong constraint on scientific hypotheses regarding such regions

"If we can solve the forward problem, we can solve the inverse problem." (!)

Next Generation Radio Occultation Instrument

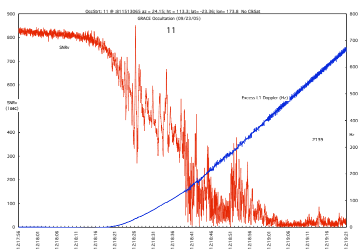

New Obs Types

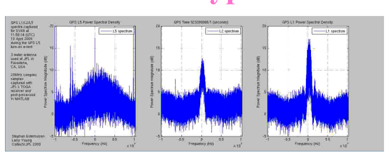

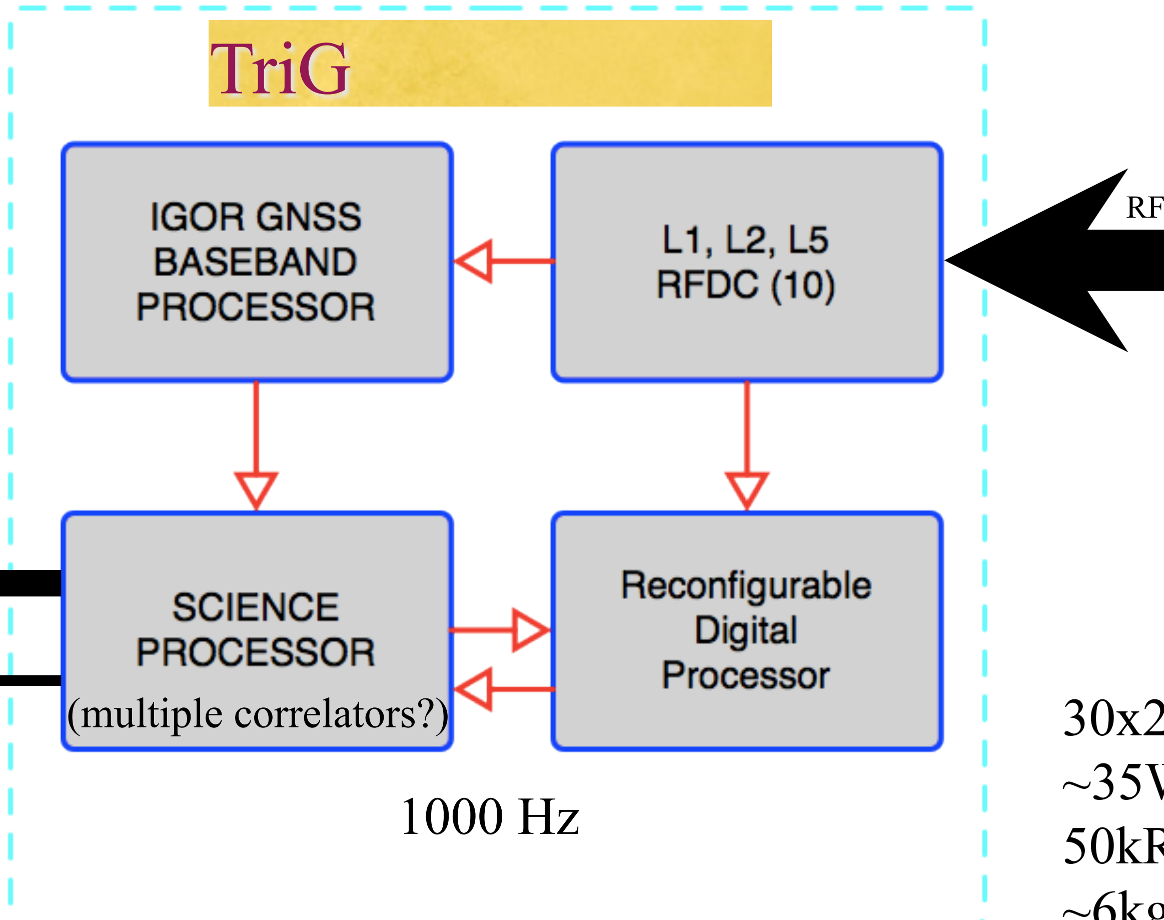

BIG
RF from Antennas

30x20x20 cm
~35W
50kRad
~6kg + Antennas

4 processors total: 2 CPU, 2 FPGA

Summary

- What is the revolution? Integrating radio occultation information content into a combined retrieval
- We have tools to make significant progress now
- Critical to increase depth penetration
  - SNR and multiple correlation
- Long term "vision": increase fraction of computer time spent doing retrievals
  - Measurements with increased sensitivity (higher spatial resolution, additional radar frequencies, camera angles, wavelengths, etc.)
  - Retrievals with increased physical content
- GNSS systems are proliferating: GPS, Galileo, GLONASS – 3x number of measurements

Hierarchical Retrieval Approaches

- **Despite all the structure in the signal, one can smooth the data to obtain meaningful results in specific limits**
  - **Doppler shift from phase rate: bending angle**
  - **Spectral content: multiple bending angles**
  - **Integral transforms: decomposition into unique bending angle for each impact parameter**
  - **Spherical symmetry: bending angle to refractivity**
  - **Spherical *asymmetry*: input impact parameter ≠ output impact parameter**

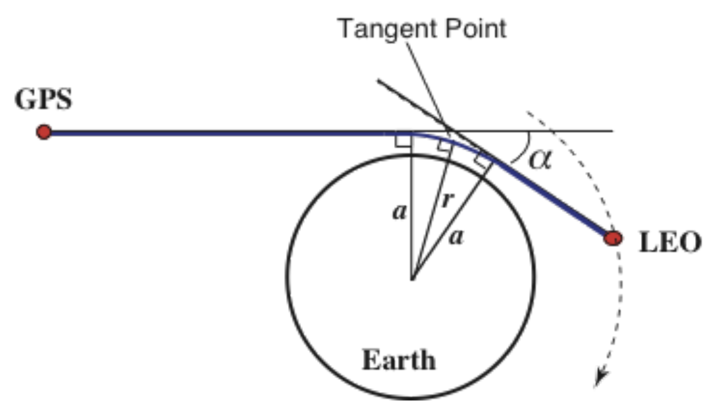

Atmospheric Multipath

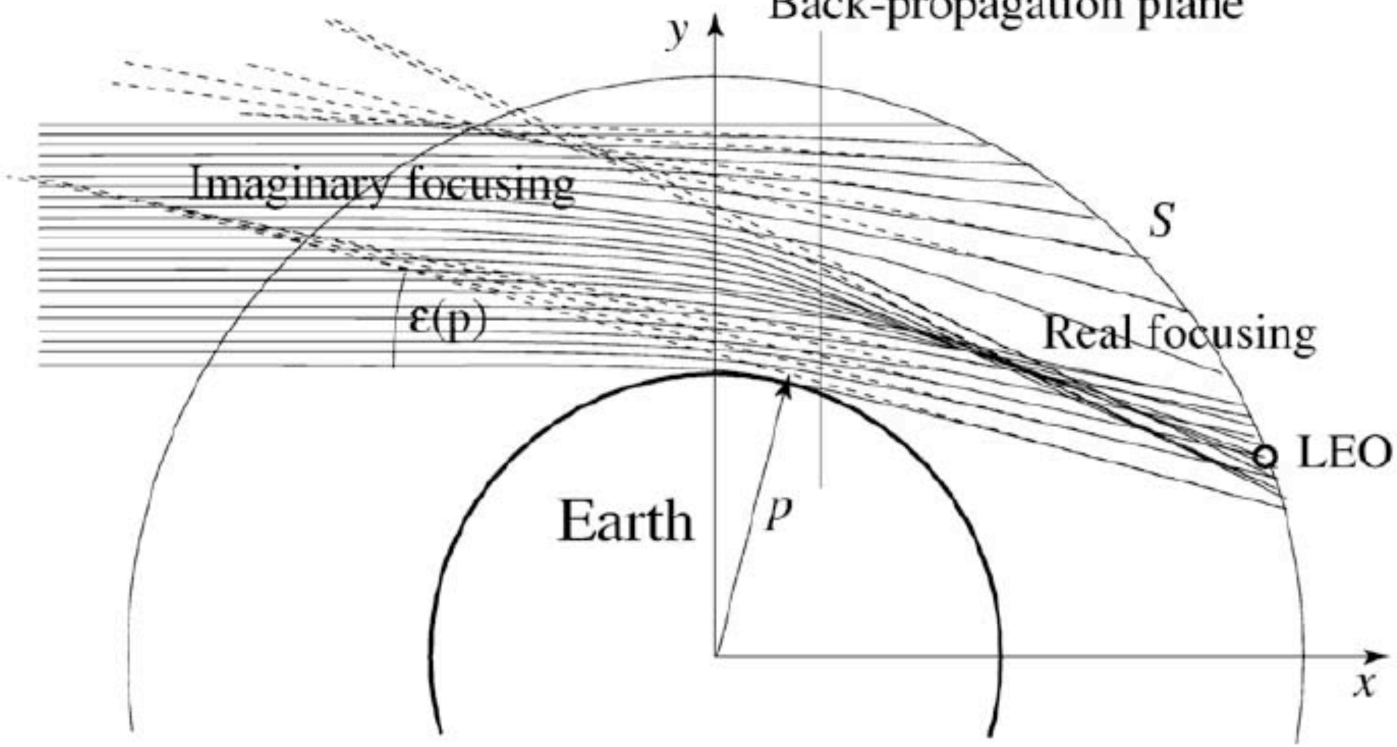

Figure 1. The geometry of multipath propagation.